



Synthesis, ADME, docking studies and *in vivo* anti-hyperglycaemic potential estimation of novel Schiff base derivatives from octadec-9-enoic acid

Garima Kapoor^{a,*}, Dharam Pal Pathak^a, Rubina Bhutani^a, Asif Husain^b, Sandeep Jain^c,
Md. Azhar Iqbal^b

^a Department of Pharmaceutical Chemistry, Delhi Institute of Pharmaceutical Sciences and Research, New Delhi, India

^b Department of Pharmaceutical Chemistry, Faculty of Pharmacy, Jamia Hamdard (Hamdard University), New Delhi, India

^c Department of Pharmaceutical Chemistry, Guru Jambheshwar University of Science and Technology, Hisar, Haryana, India

ARTICLE INFO

Keywords:

Fatty acids
Hyperglycaemia
Molecular docking
PPAR
Schiff base
STZ

ABSTRACT

A new series of octadec-9-enoic acid schiff base entities (**S1-S30**) were designed and synthesized targeting peroxisome proliferator activated receptor-gamma for agonist action. Molinspiration software (online) was used to estimate drug like molecular properties of the metabolites. Docking disquisition on co-crystallized protein of PPAR- γ (PDB ID 1FM9) was carried out which showed **S21**, **S10** and **S7** as best situated in the vital sites of receptor having docking scores -9.19 , -8.68 and -8.64 respectively. Free binding energy measured using model of Maestro 9.0 and was in range of from -40.01 and -80.54 kcal/mol, significant when compared with pioglitazone (-51.58 Kcal/mol). Seven best docked derivatives were assessed for in-vivo oral glucose tolerance on normal rats and anti-hyperglycaemic activity by streptozotocin induced diabetes model. **S21** unveiled to be the best measured analogue among all the synthesized entities. Encouraging outcomes motivates fatty acids for further development of more effective and safer compounds.

1. Introduction

Diabetes Mellitus type 2 or Non-Insulin dependent Diabetes Mellitus (NIDDM) is long-term metabolic disease [1] which is 4th ruling cause of death in world; and execution of which requires wide financial and public responsibility [2]. The International Diabetes Federation (IDF) has assessed that the world over ubiquity of diabetes has forecasted to rise from 415 million today to 642 million in 2040 [3]. In diabetes, there is imbalance in carbohydrate and lipid metabolism by insulin. Insulin is secreted from pancreatic beta cells in reaction to rising plasma glucose, with various factors reorganizing its secretion [4]. The increase in glucose level characterized by T2DM assists spreading of complications and result in metabolic abnormalities. Chronic hyperglycemia brings various disorders related to heart, kidney and eyes [5].

Recently peroxisome proliferator activated receptors (PPARs) have appeared to be one of the key governors of the nutrient and gene synergic reactions. PPARs exist in three subtypes α , β and γ , in different species. They are a group of nuclear hormone receptor isoform that manages dietary fat and are also a goal for the development of therapy for type 2 diabetes, obesity and cardiovascular disease. They also control the expression of genes involved in lipid balance and activates gene transcription to variety of drugs and natural fatty acids [5]. PPARs

are target for structurally diverse fatty acids, eicosanoids and hypolipidemic drugs [7,8].

Fatty acids are significant nutritive and healthy component implicated in heart and metabolic diseases [9]. Diets rich in stearic acid and other saturated fatty acids are favourable for diabetes mellitus patients [10]. Oleic and linoleic acids innervate insulin secretion in high-glucose concentrations which specify that free fatty acids (FFAs) rise glucose-stimulated insulin secretion (GSIS) [4]. Newly designed fatty acids work on gene expression by binding to and triggering PPAR subtypes to fall off blood glucose level [6]. Derivatives of stearic acid like bromstearate induced marked hypoglycaemia in intact animals, normalized hyperglycemia in rats with alloxan induced diabetes for 24 h after administration as when given by intra peritoneal injection, they inhibited the oxidation of fatty acids and gluconeogenesis and enhanced the glucose oxidation in intact animals and in rats with diabetes. Inhibitors of fatty acid oxidation are suggested for the pathogenesis therapy of diabetes [11]. Substituted fatty acids and its derivatives having long-chain stimulate PPAR gamma to a some extend and act as their endogenous ligand [12]. Nitro fatty acids which contain nitro groups have distinguished PPAR ligand property exhibiting particular PPAR interactions of electrophilic fatty acids [13].

Schiff bases are also a remarkable class of ligands in pharmaceutical

* Corresponding author at: Department of Pharmaceutical Chemistry, Delhi Institute of Pharmaceutical Sciences and Research, New Delhi 110017, India.

E-mail address: kapoor27garima@gmail.com (G. Kapoor).

<https://doi.org/10.1016/j.bioorg.2018.12.004>

Received 19 September 2018; Received in revised form 28 November 2018; Accepted 3 December 2018

Available online 04 December 2018

0045-2068/ © 2018 Elsevier Inc. All rights reserved.

chemistry field having synthetic flexibility, constructional resemblance with natural organic molecules and also because of imine group (N=CH–) which explains the mechanism of transformation and racemisation reaction in biological system [14]. They exhibit many pharmacological functions inclusive of antibacterial [15,16], antifungal [16], anti-diabetic [17,18], antitumor [19], anti-cancer [20], herbicidal [21], and anti-inflammatory [22] activities. Schiff bases are also used as raw material in the industries [23,24]. Schiff base ligands have shown PTP1B inhibition potential pursuing to develop as novel anti-diabetic drugs [17]. The Schiff base derivative synthesized from 3-hydroxyflavone and metformin resulted in good anti-diabetic activity, establishing new complexes decreasing primary and secondary complications of type 2 diabetes mellitus [18].

In view of aforementioned points, increasing diabetic population and side effects associated with them, we have looked into the importance and significance of natural component like fatty acid, its derivatives and schiff base derivatives in treating type II diabetes in particular, which inspired us to schedule the present organized study accommodating heterocyclic schiff base derivatives of fatty acid, expecting superior antihyperglycemic products with fewer unwanted secondary effects than the prevailing ones.

2. Material and methods

2.1. General

The reagents and solvents were purchased from commercial merchandisers like Merck, Sigma-Aldrich etc. which were taken for reactions without refining them further. The advancement of the reactions was verified by thin layer chromatography (TLC) on precoated aluminium sheet plates (Merck, Germany) at 254 nm using UV–visualizer and iodine chamber as detectors of spots on it. Melting points of the synthesized derivatives were calculated by open capillary method working on Icon- Instruments electric melting point apparatus and were not corrected. Infrared (IR) spectra were analysed by Bruker ATR spectrophotometer. Nuclear magnetic resonance (NMR), ^1H (300 MHz) and ^{13}C NMR (75 MHz) spectra of all the prepared analogues were recorded on a Bruker Advance II spectrometer DPX 300 in CDCl_3 or $\text{DMSO}-d_6$ as solvent. Tetramethyl silane (TMS) was used as internal standard and chemical shifts were indicated as δ values which were reported in parts per million (ppm). The mass spectrometric data of the series (at room temperature) were resolved on LCMS/LCQ of Agilent, Advantage-Max mass spectrophotometer. Elemental analysis was executed by Perkin-Elmer 240 elemental analyzer for C, H and N elements of each derived congener and results were in range of $\pm 0.4\%$ when compared with theoretical values. The protocol for synthetic procedure and different substitutions are summarized in Scheme 1.

2.2. Synthesis

2.2.1. Synthesis of methyl oleate (1) [6]

Oleic acid or (E)-octadec-9-enoic acid (0.25 M) and methanol (1.24 M) were taken in and poured in a three neck 250 mL round bottom flask. This round bottom flask was assembled on ice box and magnetic stirrer. 2 mL of H_2SO_4 was added drop by drop by separating funnel into it while stirring. After H_2SO_4 is finished, the mixture was refluxed for 7 h on water bath in which condenser was fixed with a glass tube containing Na_2SO_4 anhydrous and cotton at the end. The product obtained was vaporized for elimination of solvent and methanol using rotary evaporator. 100 mL of *n*-hexane was added to the residue and then washed 3 times with water. Na_2SO_4 anhydrous was added to the resulting solution and kept for 24 h before filtering. Then the residue was again purified using rotary evaporator to evaporate *n*-hexane and gave methyl oleate as a product in liquid form.

The yield of methyl oleate was 91%, m.p. 15 °C and b.p. 358 °C, IR: (KBr, cm^{-1}) 2925, 2854 (C–H), 1742 (C=O), 1658 (C=C), 1169

(C–OC), 722 $[(\text{CH}_2)_n]$. ^1H NMR: (CDCl_3 , δ , ppm): 5.31 (2H, m, CH=CH), 3.7 (3H, s, OCH_3), 2.4 (2H, t, CH_2), 1.89 (4H, m, $2 \times \text{CH}_2$), 1.6 (2H, m, CH_2), 1.29 (20H, m, $10 \times \text{CH}_2$), 0.89 (3H, s, CH_3). ESI-MS: m/z 297 (M+H). Anal. calcd. for $\text{C}_{19}\text{H}_{36}\text{O}_2$: C, 76.97; H, 12.24%. Found: C, 76.53; H, 12.56%.

2.2.2. Synthesis of stearohydrazide (2)

Methyl oleate (0.1 M) was poured in the 100 mL RBF having 80% hydrazine hydrate (0.1 M) which was refluxed with stirring for 9 h using ethanol as solvent. The resultant mixture was taken in a beaker and precipitate was obtained by keeping the beaker on ice box for few minutes and then was filtered. The recrystallization was done from ethanol to get stearohydrazide [6,25]. The yield was 84%, m.p. 107 °C, IR: (KBr, cm^{-1}) 3316–3100 (NH–NH₂), 2921, 2853 (C–H), 1629 (O=C–NH), 1160 (C–O–C), 720 $[(\text{CH}_2)_n]$. ^1H NMR: (CDCl_3 , δ , ppm): 8.38 (1H, s, NH), 3.75 (2H, s, NH₂), 2.31 (2H, t, CH_2 -CONH), 1.62 (2H, m, CH_2CH_2 -CO), 1.27 (28H, s, $14 \times \text{CH}_2$), 0.91 (3H, t, CH_3). ESI-MS: m/z 299 (M+H). Anal. calcd. for $\text{C}_{18}\text{H}_{38}\text{N}_2\text{O}$: C, 72.42; H, 12.83; N, 9.38%. Found: C, 72.71; H, 12.29; N, 9.49%.

2.2.3. General procedure for the preparation of Schiff bases (S1-S30)

To the solution of (2) (0.1 M) in 20 mL ethanol, an appropriate aldehyde (0.1 M) was added. 3 mL of glacial acetic acid was added to this mixture and then refluxed with continuous stirring for about 8 h on Parallel synthesizer. The solvent was evaporated and the mixture was poured onto crushed ice. The precipitate thus obtained was then filtered and washed with ice cold water. The resultant residue was recrystallized from benzene to give final schiff bases derivatives (S1-S30) [26,27].

2.2.3.1. *N'*-(4-hydroxybenzylidene)stearohydrazide (S1). Yield: 59%, m.p.: 274–276 °C, IR: (KBr, cm^{-1}) 2856 (RCH₃), 2925 (C–H phenyl), 1621 (C=O amide), 1482 (C=C phenyl) 1667 (–N=CH). ^1H NMR: (CDCl_3 , δ , ppm): 0.86 (3H, t, CH_3), 1.23 (28H, s, $14 \times \text{CH}_2$), 1.51–1.55 (2H, m, CH_2), 2.15 (2H, t, CH_2), 5.32 (1H, s, –OH), 6.83 [2H, d, $2 \times \text{CH}(\text{Ar})$], 7.47 [2H, d, $2 \times \text{CH}(\text{Ar})$], 7.86 (1H, s, –NH), 8.04 (1H, s, N=CH). ^{13}C NMR: ($\text{DMSO}-d_6$, δ , ppm): 14.1, 22.8, 26.0, 29.4, 29.6, 29.7, 31.9, 38.5, 116.0, 126.4, 130.6, 143.0, 160.8, 167.5. ESI-MS: m/z 403 (M+H); Anal. calcd. for $\text{C}_{25}\text{H}_{42}\text{N}_2\text{O}_2$: C, 74.29; H, 10.80; N, 6.96%. Found: C, 74.29; H, 10.80; N, 6.67%.

2.2.3.2. *N'*-(3-hydroxybenzylidene)stearohydrazide (S2). Yield: 51%, m.p.: 285–288 °C, IR: (KBr, cm^{-1}) 2854 (R-CH₃), 2923 (C–H phenyl), 1620 (C=O amide), 1479 (C=C phenyl) 1668 (–N=CH). ^1H NMR: (CDCl_3 , δ , ppm): 0.90 (3H, t, CH_3), 1.31 (28H, m, $14 \times \text{CH}_2$), 1.44–1.53 (2H, m, CH_2), 2.11 (2H, t, CH_2), 5.01 (1H, s, –OH), 6.67 [1H, d, $\text{CH}(\text{Ar})$], 7.01–7.3 [3H, m, $3 \times \text{CH}(\text{Ar})$], 7.99 (1H, s, –NH), 8.1 (H, s, N=CH). ^{13}C NMR: ($\text{DMSO}-d_6$, δ , ppm): 14.1, 22.8, 26.0, 29.4, 29.6, 29.7, 31.9, 38.5, 115.0, 118.2, 121.8, 130.3, 135.8, 143.0, 158.6, 167.5. ESI-MS: m/z 403 (M+H). Anal. calcd. for $\text{C}_{25}\text{H}_{42}\text{N}_2\text{O}_2$: C, 74.54; H, 10.51; N, 6.96%. Found: C, 74.28; H, 10.90; N, 6.72%.

2.2.3.3. *N'*-(2-hydroxybenzylidene)stearohydrazide (S3). Yield: 66%, m.p.: 262–264 °C, IR: (KBr, cm^{-1}) 2866 (R-CH₃), 2919 (C–H phenyl), 1620 (C=O amide), 1480 (C=C phenyl) 1666 (–N=CH). ^1H NMR: (CDCl_3 , δ , ppm): 0.85 (3H, t, CH_3), 1.24 (28H, s, $14 \times \text{CH}_2$), 1.53–1.64 (2H, m, CH_2), 2.18 (2H, t, CH_2), 5.32 (1H, s, –OH), 6.78–6.85 [2H, m, $2 \times \text{CH}(\text{Ar})$], 7.05–7.13 [H, m, $\text{CH}(\text{Ar})$], 7.21–7.33 [H, m, $\text{CH}(\text{Ar})$], 7.88 (1H, s, –NH), 8.07 (H, s, N=CH). ^{13}C NMR: ($\text{DMSO}-d_6$, δ , ppm): 14.1, 22.8, 26.0, 29.4, 29.6, 29.7, 31.9, 38.5, 116.0, 118.5, 121.5, 130.6, 143.0, 161.1, 167.5. ESI-MS: m/z 403 (M+H). Anal. calcd. for $\text{C}_{25}\text{H}_{42}\text{N}_2\text{O}_2$: C, 74.54; H, 10.51; N, 6.96%. Found: C, 74.18; H, 10.80; N, 6.73%.

2.2.3.4. *N'*-(3,4,5-trimethoxybenzylidene)stearohydrazide (S4). Yield: 58%, m.p.: 275–277 °C, IR: (KBr, cm^{-1}) 2865 (R-CH₃), 3001 (C–H

7.0–7.2 [(2H, m, 2xCH–(Ar))], 7.85 (1H, s, –NH), 8.03 (1H, s, N=CH). ¹³C NMR: (DMSO-*d*₆, δ, ppm): 14.1, 22.8, 26.0, 29.4, 29.6, 29.7, 31.9, 38.5, 56.2, 114.8, 117.0, 122.9, 127.4, 143.0, 148.0, 151.5, 167.5. **ESI-MS**: *m/z* 432 (M+H). Anal. calcd. for C₂₆H₄₄N₂O₃: C, 72.18; H, 10.25; N, 6.48%. Found: C, 72.55; H, 10.61; N, 6.12%.

2.2.3.7. N'-(4-(dimethylamino)benzylidene)stearohydrazide (S7). Yield: 46%, m.p.: 279–281 °C, **IR**: (KBr, cm⁻¹) 2888 (R-CH₃), 2976 (C–H phenyl), 1621 (C=O amide), 1470 (C=C phenyl) 1665 (–N=CH). ¹H NMR: (CDCl₃, δ, ppm): 0.95 (3H, t, CH₃), 1.24 (28H, s, 14xCH₂), 1.51–1.55 (2H, m, CH₂), 2.18 (2H, t, CH₂), 2.85 (6H, s, 2x-NCH₃), 6.61–6.79 [(2H, m, CH–(Ar))], 7.34–7.41 [(2H, m, 2xCH–(Ar))], 7.99 (1H, s, –NH), 8.1 (1H, s, N=CH). ¹³C NMR: (DMSO-*d*₆, δ, ppm): 14.1, 22.8, 26.0, 29.4, 29.6, 29.7, 31.9, 38.5, 40.3, 114.4, 123.3, 130.1, 143.0, 151.9, 167.5. **ESI-MS**: *m/z* 430 (M+H). Anal. calcd. for C₂₇H₄₇N₃O: C, 75.47; H, 11.03; N, 9.79%. Found: C, 75.09; H, 11.39; N, 9.48%.

2.2.3.8. N'-(furan-2-ylmethylene)stearohydrazide (S8). Yield: 58%, m.p.: 287–289 °C, **IR**: (KBr, cm⁻¹) 2878 (R-CH₃), 2989 (C–H phenyl), 1625 (C=O amide), 1470 (C=C phenyl) 1665 (–N=CH). ¹H NMR: (CDCl₃, δ, ppm): 0.91 (3H, t, CH₃), 1.27 (28H, s, 14xCH₂), 1.51–1.54 (2H, m, CH₂), 2.13 (2H, t, CH₂), 6.31–6.49 [(2H, m, CH–(Ar))], 7.09 (1H, s, –NH), 7.31–7.42 [(H, m, –OCH(furan))], 7.5 (1H, s, N=CH). ¹³C NMR: (DMSO-*d*₆, δ, ppm): 14.1, 22.8, 26.0, 29.4, 29.6, 29.7, 31.9, 38.5, 109.4, 109.9, 134.7, 143.9, 149.1, 167.5. **ESI-MS**: *m/z* 377 (M+H). Anal. calcd. for C₂₃H₄₀N₂O₂: C, 73.36; H, 10.71; N, 7.44%. Found: C, 73.33; H, 10.41; N, 7.04%.

2.2.3.9. N'-(2,4-dimethylbenzylidene)stearohydrazide (S9). Yield: 57%, m.p.: 255–257 °C, **IR**: (KBr, cm⁻¹) 2678 (R-CH₃), 2990 (C–H phenyl), 1598 (C=O amide), 1476 (C=C phenyl) 1666 (–N=CH). ¹H NMR: (CDCl₃, δ, ppm): 0.89 (3H, t, CH₃), 1.23 (28H, s, 14xCH₂), 1.51–1.56 (2H, m, CH₂), 2.1 (2H, t, CH₂), 2.33 (6H, s, 2xAr-CH₃), 6.9–6.98 [(2H, m, CH–(Ar))], 7.39–7.44 [(1H, m, CH–(Ar))], 8.02 (1H, s, –NH), 8.3 (1H, s, N=CH). ¹³C NMR: (DMSO-*d*₆, δ, ppm): 14.1, 18.2, 22.8, 24.6, 26.0, 29.4, 29.6, 29.7, 31.9, 38.5, 123.6, 126.2, 129.0, 131.0, 138.7, 140.6, 143.0, 167.5. **ESI-MS**: *m/z* 414 (M+H). Anal. calcd. for C₂₇H₄₆N₂O C, 78.20; H, 11.18; N, 6.76%. Found: C, 78.60; H, 11.39; N, 6.39%.

2.2.3.10. N'-(3-chlorobenzylidene)stearohydrazide (S10). Yield: 63%, m.p.: 270–272 °C, **IR**: (KBr, cm⁻¹) 2658 (R-CH₃), 2996 (C–H phenyl), 1628 (C=O amide), 1477 (C=C phenyl) 1668 (–N=CH). ¹H NMR: (CDCl₃, δ, ppm): 0.91 (3H, t, CH₃), 1.29 (28H, s, 14xCH₂), 1.47–1.51 (2H, m, CH₂), 2.03 (2H, t, CH₂), 6.9–7.2 [(2H, m, CH–(Ar))], 7.6–7.66 [(2H, m, 2xCH–(Ar))], 8.0 (1H, s, –NH), 8.24 (1H, s, N=CH). ¹³C NMR: (DMSO-*d*₆, δ, ppm): 14.1, 22.8, 26.0, 29.4, 29.6, 29.7, 31.9, 38.5, 127.3, 129.3, 130.3, 131.2, 134.4, 135.2, 143.0, 167.5. **ESI-MS**: *m/z* 422 (M+H). Anal. calcd. for C₂₅H₄₁ClN₂O C, 71.31; H, 9.81; N, 6.65%. Found: C, 71.20; H, 9.47; N, 6.91%.

2.2.3.11. N'-(2-chlorobenzylidene)stearohydrazide (S11). Yield: 69%, m.p.: 210–212 °C, **IR**: (KBr, cm⁻¹) 2875 (R-CH₃), 2991 (C–H phenyl), 1616 (C=O amide), 1464 (C=C phenyl) 1669 (–N=CH). ¹H NMR: (CDCl₃, δ, ppm): 0.94 (3H, t, CH₃), 1.21 (28H, s, 14xCH₂), 1.41–1.59 (2H, m, CH₂), 2.18 (2H, t, CH₂), 6.9–7.2 [(2H, m, CH–(Ar))], 7.2 [1H, d, CH–(Ar)], 7.68 [1H, d, CH–(Ar)], 7.99 (1H, s, –NH), 8.14 (1H, s, N=CH). ¹³C NMR: (DMSO-*d*₆, δ, ppm): 14.1, 22.8, 26.0, 29.4, 29.6, 29.7, 31.9, 38.5, 127.0, 129.3, 130.6, 132.5, 133.3, 143.0, 144.0, 167.5. **ESI-MS**: *m/z* 421 (M+H). Anal. calcd. for C₂₅H₄₁ClN₂O: C, 71.31; H, 9.49; N, 6.65%. Found: C, 71.19; H, 9.41; N, 6.48%.

2.2.3.12. N'-(2-bromobenzylidene)stearohydrazide (S12). Yield: 61%, m.p.: 267–269 °C, **IR**: (KBr, cm⁻¹) 2881 (R-CH₃), 2998 (C–H phenyl), 1626 (C=O amide), 1459 (C=C phenyl) 1664 (–N=CH).

¹H NMR: (CDCl₃, δ, ppm): 0.96 (3H, t, CH₃), 1.37 (28H, s, 14xCH₂), 1.49–1.51 (2H, m, CH₂), 2.08 (2H, t, CH₂), 7.2–7.28 [(2H, m, CH–(Ar))], 7.5–7.59 [2H, m, 2xCH–(Ar)], 7.88 (1H, s, –NH), 8.3 (1H, s, N=CH). ¹³C NMR: (DMSO-*d*₆, δ, ppm): 14.1, 22.8, 26.0, 29.4, 29.6, 29.7, 31.9, 38.5, 121.7, 127.9, 131.4, 131.8, 133.3, 135.3, 143.0, 167.5. **ESI-MS**: *m/z* 466 (M+H). Anal. calcd. for C₂₅H₄₁BrN₂O: C, 64.50; H, 8.88; N, 6.02%. Found: C, 64.17; H, 8.96; N, 6.35%.

2.2.3.13. N'-(3-methoxybenzylidene)stearohydrazide (S13). Yield: 51%, m.p.: 224–226 °C, **IR**: (KBr, cm⁻¹) 2875 (R-CH₃), 2998 (C–H phenyl), 1636 (C=O amide), 1461 (C=C phenyl) 1663 (–N=CH), 1265 (–OCH₃). ¹H NMR: (CDCl₃, δ, ppm): 0.86 (3H, t, CH₃), 1.34 (28H, s, 14xCH₂), 1.58–1.77 (2H, m, CH₂), 2.18 (2H, t, CH₂), 3.64 (3H, s, –OCH₃), 6.56–6.66 [(1H, m, CH–(Ar))], 7.1–7.3 [(2H, m, 2xCH–(Ar))], 7.95 (1H, s, –NH), 8.13 (1H, s, N=CH). ¹³C NMR: (DMSO-*d*₆, δ, ppm): 14.1, 22.8, 26.0, 29.4, 29.6, 29.7, 31.9, 38.5, 55.9, 113.4, 116.6, 121.5, 129.9, 134.8, 143.0, 148.0, 160.8, 167.5. **ESI-MS**: *m/z* 417 (M+H). Anal. calcd. for C₂₆H₄₄N₂O₂: C, 74.95; H, 10.64; N, 6.72%. Found: C, 74.57; H, 10.29; N, 6.94%.

2.2.3.14. N'-(2-nitrobenzylidene)stearohydrazide (S14). Yield: 67%, m.p.: 241–243 °C, **IR**: (KBr, cm⁻¹) 2768 (R-CH₃), 3006 (C–H phenyl), 1668 (C=O amide), 1471 (C=C phenyl) 1667 (–N=CH). ¹H NMR: (CDCl₃, δ, ppm): 0.95 (3H, t, CH₃), 1.23 (28H, s, 14xCH₂), 1.59–1.66 (2H, m, CH₂), 2.5 (2H, t, CH₂), 7.89–7.92 [(3H, m, 3xCH–(Ar))], 7.95–8.01 [(1H, m, CH–(Ar))], 8.28 (1H, s, –NH), 8.39 (1H, s, N=CH). ¹³C NMR: (DMSO-*d*₆, δ, ppm): 14.1, 22.8, 26.0, 29.4, 29.6, 29.7, 31.9, 38.5, 121.2, 126.3, 130.1, 132.0, 135.0, 143.0, 148.9, 167.5. **ESI-MS**: *m/z* 432 (M+H). Anal. calcd. for C₂₅H₄₁N₃O₃: C, 69.57; H, 9.57; N, 9.74%. Found: C, 69.22; H, 9.81; N, 9.45%.

2.2.3.15. N'-(2-methylbenzylidene)stearohydrazide (S15). Yield: 52%, m.p.: 248–250 °C, **IR**: (KBr, cm⁻¹) 2778 (R-CH₃), 2999 (C–H phenyl), 1638 (C=O amide), 1466 (C=C phenyl) 1669 (–N=CH). ¹H NMR: (CDCl₃, δ, ppm): 0.92 (3H, t, CH₃), 1.13 (28H, s, 14xCH₂), 1.56–1.64 (2H, m, CH₂), 2.1 (2H, t, CH₂), 2.45 (3H, s, Ar-CH₃), 6.9–7.01 [(2H, m, CH–(Ar))], 7.37–7.41 [(1H, m, CH–(Ar))], 7.92 (1H, s, –NH), 8.1 (1H, s, N=CH). ¹³C NMR: (DMSO-*d*₆, δ, ppm): 14.1, 17.9, 22.8, 24.6, 26.0, 29.4, 29.6, 29.7, 31.9, 38.5, 125.9, 126.6, 129.1, 129.2, 131.0, 138.8, 143.0, 167.5. **ESI-MS**: *m/z* 401 (M+H). Anal. calcd. for C₂₆H₄₄N₂O C, 77.94; H, 11.07; N, 6.99%. Found: C, 77.63; H, 11.32; N, 6.68%.

2.2.3.16. N'-(4-chlorobenzylidene)stearohydrazide (S16). Yield: 65%, m.p.: 291–293 °C, **IR**: (KBr, cm⁻¹) 2618 (R-CH₃), 3016 (C–H phenyl), 1636 (C=O amide), 1444 (C=C phenyl) 1665 (–N=CH). ¹H NMR: (CDCl₃, δ, ppm): 0.87 (3H, t, CH₃), 1.26 (28H, s, 14xCH₂), 1.47–1.58 (2H, m, CH₂), 2.19 (2H, t, CH₂), 7.16–7.29 [(2H, m, 2xCH–(Ar))], 7.59–7.61 [2H, m, CH–(Ar)], 7.86 (1H, s, –NH), 8.1 (1H, s, N=CH). ¹³C NMR: (DMSO-*d*₆, δ, ppm): 14.1, 22.8, 26.0, 29.4, 29.6, 29.7, 31.9, 38.5, 129.0, 130.6, 131.9, 136.6, 143.0, 167.5. **ESI-MS**: *m/z* 422 (M+H). Anal. calcd. for C₂₅H₄₁ClN₂O: C, 71.31; H, 9.81; N, 6.65%. Found: C, 71.70; H, 9.48; N, 6.39%.

2.2.3.17. N'-(4-fluorobenzylidene)stearohydrazide (S17). Yield: 61%, m.p.: 288–290 °C, **IR**: (KBr, cm⁻¹) 2818 (R-CH₃), 2966 (C–H phenyl), 1625 (C=O amide), 1464 (C=C phenyl) 1668 (–N=CH). ¹H NMR: (CDCl₃, δ, ppm): 0.90 (3H, t, CH₃), 1.25 (28H, s, 14xCH₂), 1.67–1.75 (2H, m, CH₂), 2.34 (2H, t, CH₂), 7.06–7.17 [(2H, m, 2xCH–(Ar))], 7.62–7.7 [2H, m, CH–(Ar)], 7.86 (1H, s, –NH), 8.6 (1H, s, N=CH). ¹³C NMR: (DMSO-*d*₆, δ, ppm): 14.1, 22.8, 26.0, 29.4, 29.6, 29.7, 31.9, 38.5, 115.6, 129.4, 130.8, 143.0, 165.2, 167.5. **ESI-MS**: *m/z* 405 (M+H). Anal. calcd. for C₂₅H₄₁FN₂O: C, 74.21; H, 10.21; N, 6.92%. Found: C, 74.66; H, 10.13; N, 6.59%.

2.2.3.18. N'-(3-fluorobenzylidene)stearohydrazide (S18). Yield: 57%,

m.p.: 218–220 °C, IR: (KBr, cm^{-1}) 2724 (R-CH₃), 2969 (C–H phenyl), 1626 (C=O amide), 1444 (C=C phenyl) 1666 (–N=CH). ¹H NMR: (CDCl₃, δ , ppm): 0.87 (3H, t, CH₃), 1.25 (28H, s, 14xCH₂), 1.53–1.59 (2H, m, CH₂), 2.14 (2H, t, CH₂), 7.06–7.3 [(3H, m, 3xCH-(Ar)], 7.42–7.6 [1H, m, CH-(Ar)], 7.91 (1H, s, –NH), 8.09 (1H, s, N=CH). ¹³C NMR: (DMSO-*d*₆, δ , ppm): 14.1, 22.8, 26.0, 29.4, 29.6, 29.7, 31.9, 38.5, 114.1, 117.8, 124.8, 130.5, 135.4, 143.0, 163.0, 167.5. ESI-MS: *m/z* 405 (M+H). Anal. calcd. for C₂₅H₄₁FN₂O: C, 74.21; H, 10.21; N, 6.92%. Found: C, 74.71; H, 10.59; N, 6.56%.

2.2.3.19. *N'*-(2-fluorobenzylidene)stearohydrazide (S19). Yield: 63%, m.p.: 280–282 °C, IR: (KBr, cm^{-1}) 2674 (R-CH₃), 2989 (C–H phenyl), 1656 (C=O amide), 1464 (C=C phenyl) 1676 (–N=CH). ¹H NMR: (CDCl₃, δ , ppm): 0.93 (3H, t, CH₃), 1.39 (28H, s, 14xCH₂), 1.47–1.56 (2H, m, CH₂), 2.21 (2H, t, CH₂), 6.9–7.3 [(3H, m, 3xCH-(Ar)], 7.6 [1H, t, CH-(Ar)], 8.1 (1H, s, –NH), 8.36(1H, s, N=CH). ¹³C NMR: (DMSO-*d*₆, δ , ppm): 14.1, 22.8, 26.0, 29.4, 29.6, 29.7, 31.9, 38.5, 115.6, 118.2, 124.5, 130.8, 132.7, 143.0, 159.7, 167.5. ESI-MS: *m/z* 405 (M+H). Anal. calcd. for C₂₅H₄₁FN₂O: C, 74.21; H, 10.21; N, 6.92%. Found: C, 74.33; H, 10.60; N, 6.54%.

2.2.3.20. *N'*-(4-bromobenzylidene)stearohydrazide (S20). Yield: 61%, m.p.: 225–227 °C, IR: (KBr, cm^{-1}) 2866 (RCH₃), 2955 (C–H phenyl), 1629 (C=O amide), 1472 (C=C phenyl) 1661 (–N=CH). ¹H NMR: (CDCl₃, δ , ppm): 0.96 (3H, t, CH₃), 1.29 (28H, s, 14xCH₂), 1.43–1.57 (2H, m, CH₂), 2.12 (2H, t, CH₂), 7.5–7.67 [(4H, m, 4xCH-(Ar)], 7.86 (1H, s, –NH), 8.16(1H, s, N=CH). ¹³C NMR: (DMSO-*d*₆, δ , ppm): 14.1, 22.8, 26.0, 29.4, 29.6, 29.7, 31.9, 38.5, 125.4, 131.4, 131.8, 132.8, 143.0, 167.5. ESI-MS: *m/z* 466 (M+H). Anal. calcd. for C₂₅H₄₁BrN₂O: C, 64.50; H, 8.88; N, 6.02%. Found: C, 64.15; H, 8.49; N, 6.40%.

2.2.3.21. *N'*-(3-bromobenzylidene)stearohydrazide (S21). Yield: 54%, m.p.: 216–218 °C, IR: (KBr, cm^{-1}) 2861 (RCH₃), 2945 (C–H phenyl), 1619 (C=O amide), 1442 (C=C phenyl) 1651 (–N=CH). ¹H NMR: (CDCl₃, δ , ppm): 0.89 (3H, t, CH₃), 1.31(28H, s, 14xCH₂), 1.51–1.58 (2H, m, CH₂), 2.17 (2H, t, CH₂), 7.2–7.7 [(4H, m, 4xCH-(Ar)], 8.16 (1H, s, –NH), 8.21(1H, s, N=CH). ¹³C NMR: (DMSO-*d*₆, δ , ppm): 14.1, 22.8, 26.0, 29.4, 29.6, 29.7, 31.9, 38.5, 123.2, 128.2, 131.1, 132.7, 134.0, 136.0, 143.0, 167.5. ESI-MS: *m/z* 466 (M+H). Anal. calcd. for C₂₅H₄₁BrN₂O: C, 64.50; H, 8.88; N, 6.02%. Found: C, 64.81; H, 8.66; N, 6.31%.

2.2.3.22. *N'*-(4-methoxybenzylidene)stearohydrazide (S22). Yield: 64%, m.p.: 256–258 °C, IR: (KBr, cm^{-1}) 2769 (R-CH₃), 2996 (C–H phenyl), 1612 (C=O amide), 1461 (C=C phenyl) 1655 (–N=CH), 1266 (–OCH₃). ¹H NMR: (CDCl₃, δ , ppm): 0.91 (3H, t, CH₃), 1.29 (28H, s, 14xCH₂), 1.39–1.53 (2H, m, CH₂), 1.98–2.18 (2H, t, CH₂), 3.77 (3H, s, Ar-OCH₃), 6.8–7.1 [2H, d, 2xCH-(Ar)], 7.5 [2H, d, 2xCH-(Ar)], 7.92 (1H, s, –NH), 8.19 (1H, s, N=CH). ¹³C NMR: (DMSO-*d*₆, δ , ppm): 14.1, 22.8, 26.0, 29.4, 29.6, 29.7, 31.9, 38.5, 55.9, 114.4, 126.1, 130.2, 143.0, 163.0, 167.5. ESI-MS: *m/z* 417 (M+H). Anal. calcd. for C₂₆H₄₄N₂O₂: C, 74.95; H, 10.64; N, 6.72%. Found: C, 74.59; H, 10.28; N, 6.56%.

2.2.3.23. *N'*-(2-methoxybenzylidene)stearohydrazide (S23). Yield: 68%, m.p.: 245–247 °C, IR: (KBr, cm^{-1}) 2714 (R-CH₃), 2919 (C–H phenyl), 1616 (C=O amide), 1414 (C=C phenyl) 1676 (–N=CH). ¹H NMR: (CDCl₃, δ , ppm): 0.82 (3H, t, CH₃), 1.33 (28H, s, 14xCH₂), 1.41.56 (2H, m, CH₂), 2.14–2.33 (2H, t, CH₂), 3.73 (3H, s, Ar-OCH₃), 6.8–7.01 [2H, m, 2xCH-(Ar)], 7.2–7.66 [2H, m, 2xCH-(Ar)], 7.86 (1H, s, –NH), 8.23 (1H, s, N=CH). ¹³C NMR: (DMSO-*d*₆, δ , ppm): 14.1, 22.8, 26.0, 29.4, 29.6, 29.7, 31.9, 38.5, 55.9, 114.4, 116.9, 121.2, 130.2, 132.1, 143.0, 160.5, 167.5. ESI-MS: *m/z* 417 (M+H). Anal. calcd. for C₂₆H₄₄N₂O₂: C, 74.95; H, 10.64; N, 6.72%. Found: C, 74.56; H, 10.31; N, 6.64%.

2.2.3.24. *N'*-(2,6-dichlorobenzylidene)stearohydrazide (S24). Yield:

58%, m.p.: 214–218 °C, IR: (KBr, cm^{-1}) 2761 (RCH₃), 2985 (C–H phenyl), 1639 (C=O amide), 1449 (C=C phenyl) 1655 (–N=CH). ¹H NMR: (CDCl₃, δ , ppm): 0.89 (3H, t, CH₃), 1.27 (28H, s, 14xCH₂), 1.51–1.61 (2H, m, CH₂), 2.18–2.21 (2H, t, CH₂), 7.26–7.39 [(3H, m, 3xCH-(Ar)], 7.96 (1H, s, –NH), 8.19 (1H, s, N=CH). ¹³C NMR: (DMSO-*d*₆, δ , ppm): 14.1, 22.8, 26.0, 29.4, 29.6, 29.7, 31.9, 38.5, 127.1, 131.9, 133.9, 135.4, 143.0, 167.5. ESI-MS: *m/z* 422 (M+H). Anal. calcd. for C₂₅H₄₀Cl₂N₂O: C, 65.92; H, 8.85; N, 6.15%. Found: C, 65.59; H, 8.47; N, 6.33%.

2.2.3.25. *N'*-(3-(trifluoromethyl)benzylidene)stearohydrazide (S25). Yield: 51%, m.p.: 221–223 °C, IR: (KBr, cm^{-1}) 2801 (RCH₃), 2995 (C–H phenyl), 1632 (C=O amide), 1452 (C=C phenyl) 1652 (–N=CH). ¹H NMR: (CDCl₃, δ , ppm): 0.86 (3H, t, CH₃), 1.34 (28H, s, 14xCH₂), 1.49–1.56 (2H, m, CH₂), 2.15 (2H, t, CH₂), 7.2 [1H, t, CH-(Ar)], 7.49 [(1H, d, CH-(Ar)], 7.61 [(1H, d, CH-(Ar)], 7.82 [(1H, s, CH-(Ar)], 8.03 (1H, s, –NH), 8.11(1H, s, N=CH). ¹³C NMR: (DMSO-*d*₆, δ , ppm): 14.1, 22.8, 26.0, 29.4, 29.6, 29.7, 31.9, 38.5, 124.2, 125.6, 127.5, 129.2, 131.1, 132.5, 134.1, 143.0, 167.5. ESI-MS: *m/z* 455 (M+H). Anal. calcd. for C₂₆H₄₁F₃N₂O: C, 68.69; H, 9.09; N, 6.16%. Found: C, 68.33; H, 9.40; N, 6.51%.

2.2.3.26. *N'*-(2,4,6-trimethoxybenzylidene)stearohydrazide (S26). Yield: 54%, m.p.: 249–252 °C, IR: (KBr, cm^{-1}) 2799 (R-CH₃), 2992 (C–H phenyl), 1627 (C=O amide), 1441 (C=C phenyl) 1654 (–N=CH), 1251 (–OCH₃). ¹H NMR: (CDCl₃, δ , ppm): 0.80 (3H, t, CH₃), 1.16 (28H, s, 14xCH₂), 1.49–1.51 (2H, m, CH₂), 2.16 (2H, t, CH₂), 3.76 (9H, s, 3xAr-OCH₃), 5.93 [2H, s, 2xCH-(Ar)], 7.89 (1H, s, –NH), 8.17 (1H, s, N=CH). ¹³C NMR: (DMSO-*d*₆, δ , ppm): 14.1, 22.8, 26.0, 29.4, 29.6, 29.7, 31.9, 38.5, 55.9, 92.8, 102.7, 143.0, 162.5, 165.0, 167.5. ESI-MS: *m/z* 477 (M+H). Anal. calcd. for C₂₈H₄₈N₂O₄: C, 70.55; H, 10.15; N, 5.88%. Found: C, 70.91; H, 10.44; N, 5.59%.

2.2.3.27. *N'*-(benzylidene)stearohydrazide (S27). Yield: 61%, m.p.: 257–259 °C, IR: (KBr, cm^{-1}) 2758 (R-CH₃), 3001 (C–H phenyl), 1641 (C=O amide), 1476 (C=C phenyl) 1658 (–N=CH). ¹H NMR: (CDCl₃, δ , ppm): 0.81 (3H, t, CH₃), 1.29 (28H, s, 14xCH₂), 1.47–1.59 (2H, m, CH₂), 2.13 (2H, t, CH₂), 7.2–7.3 [(3H, m, 3xCH-(Ar)], 7.51–7.59 [(2H, m, 2xCH-(Ar)], 8.11 (1H, s, –NH), 8.2 (1H, s, N=CH). ¹³C NMR: (DMSO-*d*₆, δ , ppm): 14.1, 22.8, 26.0, 29.4, 29.6, 29.7, 31.9, 38.5, 127.3, 129.3, 130.3, 131.2, 134.4, 135.2, 143.0, 167.5. ESI-MS: *m/z* 387 (M+H). Anal. calcd. for C₂₅H₄₂N₂O: C, 77.67; H, 10.95; N, 7.25%. Found: C, 77.41; H, 10.76; N, 7.39%.

2.2.3.28. *N'*-(5-chloro-2-hydroxybenzylidene)stearohydrazide (S28). Yield: 67%, m.p.: 235–237 °C, IR: (KBr, cm^{-1}) 2796 (R-CH₃), 2914 (C–H phenyl), 1620 (C=O amide), 1475 (C=C phenyl) 1655 (–N=CH). ¹H NMR: (CDCl₃, δ , ppm): 0.87 (3H, t, CH₃), 1.24 (28H, s, 14xCH₂), 1.41–1.55 (2H, m, CH₂), 2.03 (2H, t, CH₂), 5.03 (1H, s, –OH), 6.7 [2H, d, 2xCH-(Ar)], 7.13 [1H, m, CH-(Ar)], 7.5 [H, d, CH-(Ar)], 7.98 (1H, s, –NH), 8.17 (H, s, N=CH). ¹³C NMR: (DMSO-*d*₆, δ , ppm): 14.1, 22.8, 26.0, 29.4, 29.6, 29.7, 31.9, 38.5, 117.4, 119.9, 127.0, 130.7, 132.6, 143.0, 159.2, 167.5. ESI-MS: *m/z* 438 (M+H). Anal. calcd. for C₂₅H₄₁ClN₂O₂: C, 68.70; H, 9.46; N, 6.41%. Found: C, 68.39; H, 9.07; N, 6.80%.

2.2.3.29. *N'*-(4-(diethylamino)-2-hydroxybenzylidene)stearohydrazide (S29). Yield: 53%, m.p.: 217–220 °C, IR: (KBr, cm^{-1}) 2758 (R-CH₃), 2896 (C–H phenyl), 1618 (C=O amide), 1471 (C=C phenyl) 1658 (–N=CH). ¹H NMR: (CDCl₃, δ , ppm): 0.85 (3H, t, CH₃), 1.13–1.21 [6H, m, 2xCH₃ of (diethylamino)], 1.19 (28H, s, 14xCH₂), 1.47–1.53 (2H, m, CH₂), 2.03 (2H, t, CH₂), 3.39 [4H, q, 2xCH₂ (diethylamino)], 5.03 (1H, s, –OH), 6.1–6.2 [(2H, m, 2xCH-(Ar)], 7.3 [(1H, m, CH-(Ar)], 7.9 (1H, s, –NH), 8.14 (1H, s, N=CH). ¹³C NMR: (DMSO-*d*₆, δ , ppm): 13.0, 14.1, 22.8, 26.0, 29.4, 29.6, 29.7, 31.9, 38.5, 44.7, 99.2, 107.0, 108.0, 131.5, 143.0, 153.5, 162.0, 167.5. ESI-MS: *m/z* 474 (M

+H). Anal. calcd. for $C_{29}H_{51}N_3O_2$, 73.52; H, 10.85; N, 8.87%. Found: C, 73.12; H, 10.47; N, 8.49%.

2.2.3.30. *N'*-(4-chloro-3-nitrobenzylidene)stearohydrazide (S30). Yield: 63%, m.p.: 270–272 °C, IR: (KBr, cm^{-1}) 2758 (R-CH₃), 2992 (C–H phenyl), 1628 (C=O amide), 1473 (C=C phenyl) 1658 (–N=CH). ¹H NMR: (CDCl₃, δ, ppm): 0.96 (3H, t, CH₃), 1.17 (28H, s, 14xCH₂), 1.49–1.59 (2H, m, CH₂), 2.19 (2H, t, CH₂), 7.69 [(2H, d, 2xCH-(Ar)], 8.41 [(1H, s, CH-(Ar)], 8.0 (1H, s, –NH), 8.24 (1H, s, N=CH). ¹³C NMR: (DMSO-*d*₆, δ, ppm): 14.1, 22.8, 26.0, 29.4, 29.6, 29.7, 31.9, 38.5, 125.5, 129.9, 131.2, 132.8, 136.7, 143.0, 148.9, 167.5. ESI-MS: *m/z* 467 (M+H). Anal. calcd. for $C_{25}H_{40}ClN_3O_3$, 64.43; H, 8.65; N, 9.02%. Found: C, 64.09; H, 8.28; N, 9.41%.

2.3. *In silico computational studies*

2.3.1. Physicochemical property Prediction: Lipinski rule

Physicochemical property prediction is very crucial for the drafting and synthesis of novel PPAR gamma agonists with enhanced biological profile. The drug-resemblance characters of new identities were tested by applying Lipinski's rule of five by using online Molinspiration property calculation toolkit [28]. The requirement is that the derivatives should not have more than 5 and 10 hydrogen bond donors or acceptors respectively, MW less than 500 amu, and partition coefficients value between octanol and water (log P(oct/wat)) less than 5. For the compound to be active orally, it should not violate more than one of these rules. Estimation of *mi log P*, H-bond donors, H-bond acceptors; number of rotatable bonds, molecular volume and molecular weight of the novel series designed were predicted by this toolkit. Additional basic specifications like Topological Polar Surface Area (TPSA) were also calculated to identify membrane penetration of new compounds having low CNS bioavailability to get best oral drug identities. Synthetic analogues with TPSA values > 60 Å are selected for orally active drug candidates and are chosen for developing new molecules. Aforementioned online prediction software assisted in perceiving novel collection of molecules with acceptable biological activity [29–30]. The %ABS (% Ab) value for synthesized derivatives was evaluated by putting TPSA value in the following formula: %Ab = 109 – [0.345 × TPSA] [31].

2.3.2. Molecular docking and Prime MMGBSA [29]

Docking estimations for getting binding patterns of all novel compounds was completed by using Maestro 9.0 Schrodinger program, New York, USA on PDB ID-1FM9 which is a PPAR-γ crystal captured by RCSB. The elucidations of divergent process of binding of these molecules with cavities of the receptor were reported. The effective revealed focus in anti-hyperglycaemic potential is PPAR gamma receptor. Protein data bank (PDB 1FM9) was opened and the basic crystal structure was downloaded. Tool named Lig prep was used in preparing ligands i.e. novel hybrids and protein preparation wizard in drafting structure of protein. Molecules of water which were not required were removed by software physically from the framework. The structure of protein was intensified and then its energy was minimized by root-mean-square deviation of 0.3 Å. Ligands energy was also minimized with the OPLS (optimized potentials for liquid simulations) 2005 force field. Glide scores and free binding energy of docked compounds was used in estimating binding affinities.

Software Maestro 9.0 is used to estimate binding energy of the ligands i.e. synthesized compounds and pioglitazone against receptor having PDB ID 1FM9 which is crystal structure of PPAR γ through method called as Prime molecular mechanics-generalized born surface area (MMGBSA). Conclusions can be obtained by regulating MM-GBSA program instantly from the file created by docking procedure. The perfect organization and binding resemblance of the novel entities on the vital positions of the receptor with the nearby amino acids are anticipated by docking glide score, free binding energy, H bond and pie-

pie bonding. The protein-ligand energy in coulomb-vdW is elucidated by the Emodel function.

2.4. *In vitro study*

2.4.1. PPAR-gamma transactivation assay [32]

Entities having good glide score (S4, S5, S7, S10, S14, S15 and S21) were checked for their PPAR-gamma transactivation activity. Human embryonic kidney (HEK) 293 cells were cultured in Dulbecco's Modified Eagle Medium (DMEM) with foetal bovine serum (FBS-10% heat inactivated). Cells were incubated in 5% CO₂ incubator at 37 °C till it reaches 70–80% convergence. Cells were inoculated in 96-well plates containing 60,000 cells/well. After that, they were transfected with 2.5 μL of PPRE-Luciferase, 6.67 μL of PPARγ, 1.0 μL of Renilla, and 20 μL of Lipofectamine. Five hours after transfection, cells were treated with the synthesized derivatives (10 μM) for 24 h which were then collected by cell culture lysis buffer. Luciferase activity was observed after 42 h on luminometer using the luciferase assay kit (Promega) as reported in the manufacturer's instructions. Pioglitazone was taken as standard drug.

2.4.2. Cytotoxicity study by MTT assay [33]

In vitro cytotoxicity study was performed on the selected compounds having good docking glide scores and which were found to be PPAR gamma active, in order to carry out *in vivo* study on the same. Breast cancer cell line (MCF-7) cells were plated at a density of 5×10^4 cells/mL were incubated for 48 h with different concentrations of derivatives (S4, S5, S7, S10, S14, S15 and S21) dissolved in DMSO (the final volume of DMSO/medium was less than 1% in experiments). Etoposide and DMSO were used as positive and negative controls, respectively. After this, the medium was removed and 200 μL of a phenol red-free medium containing MTT (1 mg/mL, final concentration) was added to all wells. After 4 h of incubation, the culture medium was replaced with 100 μL of DMSO to each well. The absorbance was then measured on a spectrophotometer (SpectraMax; Molecular Devices) at 570 nm. Then the cells were exposed to different concentrations of derivatives for 48 h and measurement of cell viability was taken by MTT method. The assay is based on the cleavage of the yellow tetrazolium salt MTT [3-(4,5-dimethylthiazol-2-yl)-2,5-diphenyl tetrazolium bromide] into purple formazan by metabolically active cells after reduction by mitochondrial enzymes, which can be spectrophotometrically quantified at 570 nm. The amount of formazan product generated is proportional to the number of living cells and leads to a stronger color formation. The experiment was performed for three times and the values for each were calculated from triplicate wells. IC₅₀ values were determined applying nonlinear regression analysis to the data for three dilutions.

2.5. *In vivo study*

Albino wistar rats (200–250 g) of either sex were taken from Animal House Center of Delhi Institute of Pharmaceutical Sciences and Research, New Delhi for oral glucose tolerance and anti-hyperglycaemic study. All the procured animals were divided and housed in different polypropylene cages at standard laboratory conditions (temperature 22 ± 2 °C and relative humidity $45 \pm 5\%$ with 12 h day: 12 h night cycle) maintaining disinfected state. All animals were nourished with normal pellet diet and water *ad libitum*. The study on experimental animals was performed after the approval of Institutional Animal Ethical Committee (IAEC) through protocol IAEC/2016-I/ Prot. No.05 corresponding to CPCSEA guidelines. Blood glucose level was measured using automatic analysis (Accu-Chek Active Glucose, Roche Diagnostics, Mannheim, Germany).

2.5.1. Oral glucose tolerance test in normal rats

S4, S5, S7, S10, S14, S15 and S21 entities were selected from all the synthesized derivatives for oral glucose tolerance test according to

their docking scores. The test was performed on overnight fasted normal rats, divided into nine groups, six in each. Group 1 was taken as normal and was given 0.1% (w/v) aqueous CMC solution (5 mL/kg) orally. Group 2 was marked as standard group which was treated with suspension of 36 mg/kg b.w. of pioglitazone in 0.1% (w/v) aqueous CMC. Groups 3–9 were served 100 mg/kg of the test analogs **S4**, **S5**, **S7**, **S10**, **S14**, **S15** and **S21** respectively orally using oral gavage. Glucose (5 g/kg b.w) was given 30 min post-administration of CMC, standard drug and tested compounds. Blood glucose level was measured by retro orbital plexus of rat eye at 0 h (just before), 30 min and 90 min after the oral administration of the selected test derivatives by using Accu-chek Active TM Test strips in Accu-chek Active TM Test meter of Roche [34–37].

2.5.2. Hypoglycaemic activity on streptozotocin-induced diabetic rats [38–42]

2.5.2.1. Drugs used. Pioglitazone was specified to rats in quantity of 36 mg/kg body weight in 0.1% (w/v) aqueous CMC which is stated as a reference standard.

2.5.2.2. Induction of non-insulin dependent diabetes mellitus. The non-insulin-dependent diabetes mellitus was created in overnight fasted rats, by intraperitoneal injection of freshly made streptozotocin solution in 0.1 M citrate buffer (4.5pH) at a dose of 60 mg/kg body weight. After this regiment, blood glucose level was observed after 48 h to check hyperglycaemia. Diabetes was evolved and stabilized for 2 days and then anti-diabetic study was done. The rats having permanent blood glucose level > 250 mg/dL were accounted to be diabetic and were used in further study [35].

2.5.2.3. Group design. **S4**, **S5**, **S7**, **S10**, **S14**, **S15** and **S21** compounds were selected for the study by evaluating their docking results. In this, the rats were divided into nine groups (n = 6) after NIDDM induction. Group 1 taken as diabetic control (0.1% (w/v) aqueous CMC solution, 5 mL/kg b.w.), Group 2 served as reference standard received pioglitazone, 36 mg/kg b.w. by oral route, suspended in 0.1% (w/v) aqueous CMC vehicle. Group 3–9 taken as test groups, received oral dose of 100 mg/kg b.w. of selected test derivatives **S4**, **S5**, **S7**, **S10**, **S14**, **S15** and **S21** respectively through oral gavage.

2.5.2.4. Blood glucose measurement. Blood sample was collected from retro orbital plexus of the eye under light ether anaesthesia using capillary tube and recorded at an interval of 0, 2, 4, and 6 h gap by Accu-chek Active TM Test strips in Accu-chek Active TM Test meter of Roche.

2.5.3. Statistical analysis

Results of both the studies are expressed as means \pm SEM for groups. Difference between data of derivatives and control were tested by one-way analysis of variance ANOVA followed by dunnett's comparison test. The values were taken to be significant at $p < 0.05$ and $p < 0.01$.

3. Results and discussion

3.1. Chemistry

New Schiff base analogs of fatty acid showing agonism to PPAR were drafted and prepared by Scheme 1. Stearohydrazide (2) required as starting material for derivatives was obtained from methyl oleate (1) which was acquired from the reaction of hydrazine hydrate. To the solution of stearohydrazide in ethanol, glacial acetic acid was added and refluxed with vigorous stirring with appropriate substituted aldehydes to give respective novel chemical schiff base entities (**S1**–**S30**). The structures of synthesized derivatives **S1**–**S30** were characterized by proton and carbon nuclear magnetic resonance and MASS spectroscopy.

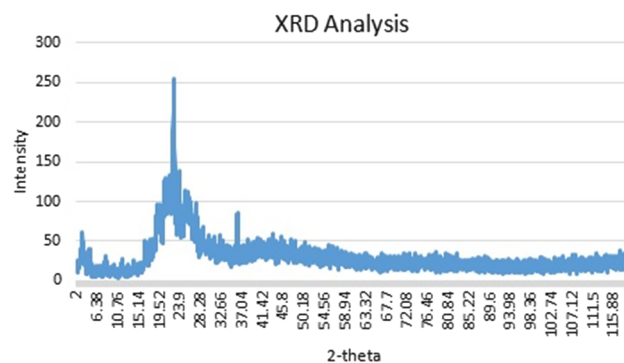


Fig. 1. X-ray analysis of **S21**.

The IR spectra developed bands in range of 1598–1656 (C=O amide) and 1651–1676 (–N=CH). The ^1H NMR spectrum showed singlet at 7.5–8.39 parts per million for protons of –N=CH. δ value for the same was around 143.0 parts per million in ^{13}C NMR spectra. Almost all derivatives displayed weak molecular ion peaks reporting instability of ions. Elemental analysis data were found in the range of $\pm 0.4\%$ for the theoretical values of the analyzed elements (C, H, N).

The X-ray analysis of the compound **S21** was done by Rigaku Ultima IV X-ray Diffractometer (Fig. 1).

3.2. Computational study

3.2.1. In silico pharmacokinetic prediction

Prediction of Absorption, Distribution, Metabolism and Excretion by Molinspiration of novel synthesized schiff bases (**S1**–**S30**) are represented in Table 1. For a drug to be active orally, it should not violate more than one of Lipinski rules. In this study all the tested synthetic entities pass the Lipinski screening test. The topological polar surface area values of our synthesized compounds are from 41.46 to 87.29 Å, which engross additional structural elaboration for the evolution of new analogues. Absorption percentage (% ABS) is found to be in range of 78.88 to 94.69 which shows that all the derivatives have moderate to good permeability into membrane.

3.2.2. Molecular docking

Molecular Docking has been reported for getting the binding patterns of novel compounds with the vital positions of 3D PPAR- γ crystal form which was taken from protein data bank (PDB ID-1FM9) having similarity with enzymes of humans. The work was completed by using by Maestro 9.0 Schrodinger program. Glide scores and free binding energies of all entities are shown in Table 2. **S21**, **S10** and **S7** were showing best scores as –9.19, –8.68 and –8.64 respectively, thus are well positioned on the sites as compared to the standard pioglitazone having docking score of –8.46. In this study we have explored binding approach of three most promising derivatives of the series (**S21**, **S10** and **S7**). Examination by molecular docking of **S21**, **S10** and **S7** into the vital locations of enzyme specified different molecular interrelationships and interactions (hydrogen bond, π -interaction, and hydrophobic interactions) for good activity and affinity of the compounds. Illustrations of binding patterns in 3D and 2D view of these best docked compounds (**S21**, **S10** and **S7**) within 3.5 Å are shown in Figs. 2–4 respectively.

Compound **S21** having highest docking score is the most effective derivative of the series. **S21** shows three hydrogen bond interactions between oxygen of –C=O group of compound and amino acid HIE 449, HIP 323 and TYR 473, in which two hydrogen bonds, HIP 323 and TYR 473 are similar to the standard drug, pioglitazone. It forms hydrophobic interaction with Ile262, Pro269, Leu270, Cys285, Leu340, Ile341, Leu330, Ile326, Phe282, Leu453, Phet363, Leu356 Ala278, Phe360, Ile281 and Leu353. The chain and aromatic ring also forms

Table 1
ADME property estimation.

Compd. code	%ABS	TPSA ^a	<i>n</i> -rotb ^b	Molecular weight	Molecular volume	Log P ^c	nOHNH ^d	nON ^e	Lipinski's violation (< / = 1)
S1	87.71	61.69	18	402.62	432.10	8.88	2	4	1
S2	87.71	61.69	18	402.62	432.10	8.87	2	4	1
S3	87.71	61.69	18	402.62	432.10	9.04	2	4	1
S4	85.13	69.16	21	476.70	500.72	8.93	1	6	1
S5	88.32	59.93	20	446.68	475.17	8.93	1	5	1
S6	84.53	70.92	19	432.65	457.64	8.80	2	5	1
S7	93.57	44.70	19	429.69	469.99	9.10	1	4	1
S8	90.16	54.60	18	376.58	405.65	8.77	1	4	1
S9	94.69	41.46	18	414.68	457.20	9.31	1	3	1
S10	94.69	41.46	18	421.07	437.62	9.27	1	3	1
S11	94.69	41.46	18	421.07	437.62	9.27	1	3	1
S12	94.69	41.46	18	465.52	441.96	9.30	1	3	1
S13	91.50	50.70	19	416.65	449.62	9.07	1	4	1
S14	78.88	87.29	19	431.62	447.41	9.03	1	6	1
S15	94.69	41.46	18	400.65	440.64	9.19	1	3	1
S16	94.69	41.46	18	421.07	437.62	9.27	1	3	1
S17	94.69	41.46	18	404.61	429.01	9.12	1	3	1
S18	94.69	41.46	18	404.61	429.01	9.11	1	3	1
S19	94.69	41.46	18	404.61	429.01	9.11	1	3	1
S20	94.69	41.46	18	465.52	441.96	9.31	1	3	1
S21	94.69	41.46	18	465.52	441.96	9.30	1	3	1
S22	91.50	50.70	19	416.65	449.62	9.08	1	4	1
S23	91.50	50.70	19	416.65	449.62	9.07	1	4	1
S24	94.69	41.46	18	455.51	451.15	9.43	1	3	1
S25	94.69	41.46	19	454.62	455.38	9.33	1	3	1
S26	85.13	69.16	21	476.70	500.72	9.07	1	6	1
S27	94.69	41.46	18	386.62	424.08	9.06	1	3	1
S28	87.71	69.16	18	437.07	495.63	9.25	2	4	1
S29	86.59	64.93	21	473.75	511.61	9.30	2	5	1
S30	78.88	87.29	19	466.07	460.95	9.24	1	6	1

^a Topological polar surface area (TPSA).

^b Number rotatable bonds (*n*-rotb).

^c Log of partition coefficient *n*-octanol/water (LogP).

^d Hydrogen bond donors (nOHNH).

^e Hydrogen bond acceptor (nON).

hydrophobic interaction via weak van der Waals interactions with side chains non-polar group of Phe287, Met348, Val339, Leu465 Ile456 and Met364. The polar interaction also takes place with Gln283, Gln271, Ser342 and Gln286. The carboxy group of chain also form hydrogen bond with Ser289, Hie449 and Tyr473 (Fig. 2).

In the derivative S10, second most active entity, showed one hydrogen bond interaction with TYR 473 amino acid which is similar to the standard drug, pioglitazone and another hydrogen bond is formed between hydrogen of –NH with MET 364 amino acid. There are formation of hydrophobic interaction with Phe360, Cys285, Phe287, Pro269, Leu270, Ile262, Ile341, Leu340, Ile326, Leu330, Tyr327, Phe282, Ile456, Leu453, Met364, Ala278, Leu353, Phe363 Ile281 and Leu356. The chain of fatty acid and aromatic ring also forms hydrophobic interaction via weak van der Waals interactions with side chains non-polar group of Val339, Leu369 and Leu465. The polar interaction also takes place with Gln283, Gln271, Ser342 and Gln286. The carboxy group of chain also form hydrogen bond with Hip323, Ser289, Hie449 and Tyr473 (Fig. 3).

Compound S7 showed three hydrogen bond interactions between oxygen of –C=O group and amino acid SER 289, HIP 323 and TYR 473 which are similar to the standard drug, pioglitazone. It has also shown many molecular interactions like hydrophobic interaction with Phe360, Leu353, Leu330, Leu333, Val339, Cys285, Ile341, Ile281, Ile249, Ile326, Leu453, Ile456, Phe363 and Leu356. The fatty acid long chain and aromatic ring also forms hydrophobic interaction via weak van der Waals interactions with side chains non-polar group of Met364, Leu340, Tyr327, Leu469, and Leu465. Pie-pie stacking takes place between phenyl ring and Phe282. The polar interaction also takes place with Gln283, Hie449 and Gln286. The carboxy group of chain also form hydrogen bond with Hip323, Ser289 and Tyr473 (Fig. 4).

3.2.3. Free binding energy (MM-GBSA)

The synthesized ligands and selected receptor protein were developed by formerly outlined procedure and before performing MM-GBSA prime free energy estimation using model Prime MMGBSA DG binds from Maestro 9.0, every molecule of water was removed. Table 2 shows the results of free binding energy stating that molecules S7, S10 and S21 fits well into the receptor PPAR-γ (1FM9). Compound S21 exhibited commendatory conformation having binding energy of –70.63 kcal/mol which is more as compared to standard drug pioglitazone (–51.58 kcal/mol). S7 and S10 were also found to show more binding free energy than standard, –65.58 and –63.86 respectively and so are more effective analogues than standard. In addition Table 2 shows that the binding energies of synthesized entities is from –40.01 and –80.54 kcal/mol and established that all molecules have remarkable potential as compared to that of standard.

3.3. Biological evaluation

3.3.1. In vitro PPAR-γ transactivation assay

Among all the synthesized compounds, derivatives having glide scores (> 8.05) in docking analysis were selected for PPAR-γ transactivation assay to indicate their mode of action when compared with reference pioglitazone having glide score 8.46. All the seven compounds S4, S5, S7, S10, S14, S15 and S21 were found to be PPAR-γ active. Derivative S21 showed best PPAR-γ activity percentage (76.14) which is even more than the standard having 75.63. Transactivation percentage of S10 (73.24) was comparable to the pioglitazone. Compounds S7, S14, S5, S4 and S15 showed 65.24, 59.2, 52.22, 51.52, and 49.41% PPAR-γ transactivation respectively as compared to reference pioglitazone with 75.63% transactivation. Results are shown in Fig. 5.

Table 2
Compounds with code, their Glide score, free binding energy and hydrogen interactions with amino acid residues.

Compound code	Glide score	Free binding energy (kcal/mol)	Hydrogen bonds		
			Atom of ligand	Amino acids	Distance (Å ⁰)
S1	-7.693	-63.74	O	GLU 259	2.91
			H	ARG 280	2.73
S2	-7.351	-55.88	O	SER 342	1.88
			H	GLU 343	1.67
S3	-8.823	-68.46	H	ARG 280	2.73
			O	SER 342	2.85
S4	-7.375	-66.29	N	SER 342	4.59
			O	SER 342	2.70
			N	SER 342	2.53
			H	GLY 284	2.50
S5	-6.929	-64.24	O	GLN 283	3.65
			O	SER 342	2.17
S6	-9.998	-72.28	GLU 343	4.44	
			N	SER 342	2.49
			H	GLY 284	2.40
S7	-9.519	-65.58	H	ARG 280	1.88
			O	SER 289	2.16
S8	-8.010	-56.21	HIP 323	2.47	
			TYR 473	3.42	
			SER 289	1.82	
			HIP 323	2.13	
			-	-	
S9	-6.921	-68.93	-	-	-
S10	-9.042	-63.86	H	PHE 360	2.31
			H	MET 364	4.18
S11	-8.096	-64.84	O	SER 342	2.45
			N	SER 342	1.50
S12	-8.362	-68.84	-	-	-
S13	-8.170	-70.41	O	SER 342	1.87
			H	GLY 284	2.45
			O	GLU 343	4.14
S14	-5.731	-63.54	O	SER 342	1.99
			LYS 265	3.62	
			GLN 283	4.16	
			H	GLU 259	2.46
S15	-7.647	-68.16	H	GLU 259	2.29
			H	LEU 270	2.50
			H	LEU 270	2.50
S16	-7.521	-64.31	O	SER 342	2.29
			H	GLU 343	4.41
			H	GLY284	2.28
S17	-8.150	-69.34	H	ARG 280	2.45
S18	-7.120	-67.81	H	GLU 259	2.42
S19	-9.535	-60.45	O	SER 289	2.01
			HIP 323	2.27	
			HIP 323	2.27	
S20	7.574	-70.36	O	SER 342	3.37
			N	SER 342	3.02
S21	-9.211	-70.63	O	HIE 449	1.89
			TYR 473	3.27	
S22	-6.592	-55.26	O	SER 342	2.24
			H	GLU 291	2.41
			N	GLU 343	3.39
S23	-8.533	-63.83	H	MET 364	3.10
			O	TYR 473	4.80
S24	-8.012	-70.59	O	SER 342	2.67
			N	SER 342	3.64
S25	-8.048	-65.06	O	SER 342	1.95
			H	GLU 343	2.52
S26	-8.264	-80.54	N	SER 342	2.46
			O	CYS 285	2.78
S27	-7.820	-69.93	O	SER 342	3.29
			H	GLU 259	2.51
			H	ARG 280	2.73
S28	-8.173	-72.14	O	SER 342	2.06
			GLU 343	3.88	
S29	-7.284	-64.80	O	GLU 343	2.18
			H	GLN 294	2.49
			H	GLU 291	1.88
S30	-5.993	-53.79	O	GLU 343	2.45
			LEU 228	2.80	
			SER 342	3.81	

Table 2 (continued)

Compound code	Glide score	Free binding energy (kcal/mol)	Hydrogen bonds		
			Atom of ligand	Amino acids	Distance (Å ⁰)
Pioglitazone	-8.46	-51.58	S	SER 289	2.560
			O	HIE 449	1.961
			O	HIP 323	2.637
				TYR 473	

3.3.2. *In vitro* cytotoxicity study

The evaluation of cytotoxicity of the seven PPAR-gamma active derivatives **S4**, **S5**, **S7**, **S10**, **S14**, **S15** and **S21** was done against the human breast cancer cell line MCF-7 by using MTT assay. From the results of the test compounds expressed as IC₅₀ values (concentration required to inhibit tumour cell proliferation by 50%) shown in Table 3, it can be demonstrated that all the seven synthesized derivatives did not indicate any cytotoxicity (IC₅₀ > 100) when compared with the standard etoposide (IC₅₀ = 12.5 ± 0.32).

3.3.3. Oral glucose tolerance test (OGTT) in normal rats

Glucose given to normal rats increased glucose level from 82.21 ± 0.57 to 168.05 ± 2.75 at 30 min and was then lowered to normal at 90 min. Administration of selected synthetic compounds improved the tolerance of glucose significantly at 90 min. The effect of the compounds remained statistically significant at 90 min. Results of the glucose tolerance test performed on normal rats are shown in Table 4 and Fig. 6. After giving glucose to rats, at 30 mins, blood glucose level raised to 168.05 and 161.85 mg/dl respectively in normal and pioglitazone group which showed a hyperglycaemic peak in graph. Administration of novel fatty acid derivatives at thirty minutes after feeding with glucose also increased the blood glucose level from 160.82 to 170.15 mg/dL range. After that, the administration of novel drugs reduced the blood glucose levels to less than that produced in control group after 90 min. At 90 min, blood glucose levels in novel derivatives-administered groups approached the level of pioglitazone-dosed group. The decrease in blood glucose level at 90 min after glucose load was most efficient in **S21**, which is found to be most active of the seven selected derivatives.

3.3.4. Antihyperglycemic evaluation in STZ induced rats

The selected synthesized fatty acid derivatives were administered to STZ-induced diabetic rats to determine the blood glucose concentrations under the diabetic condition. Changes in the blood glucose level in each group of rats were followed during a 6 h period as 0 h, 2 h, 4 h, 6 h after administration of STZ (60 mg/kg/i.p.) which is described in Table 5 and Fig. 7. The oral administration of pioglitazone (36 mg/kg b.w.) showed a significant reduction in glucose level throughout the experimental period. The administration of pioglitazone produced a significant reduction in glucose level to 124.54 mg/dL after 6 h, while for the same period of time, only a slight decrease in blood glucose level compared to control. The administration of selected derivatives (100 mg/kg b.w.) also produced a reduction in glucose level after 6 h, which is comparable to the level decreased by pioglitazone administration. **S21** is found to be most potent among all derivatives tested as it reduced the blood glucose level to 119.88 mg/dL in 6 h and standard pioglitazone reduced level of glucose to 124.54 mg/dL. **S10** and **S7** have reduced the glucose level to 130.08 and 128.55 mg/dL respectively. Compounds **S4**, **S5**, **S14** and **S15** are moderately active. Hence, all the tested candidates can be considered that further research and can be used as anti-hyperglycemic drugs with safer early onset of action.

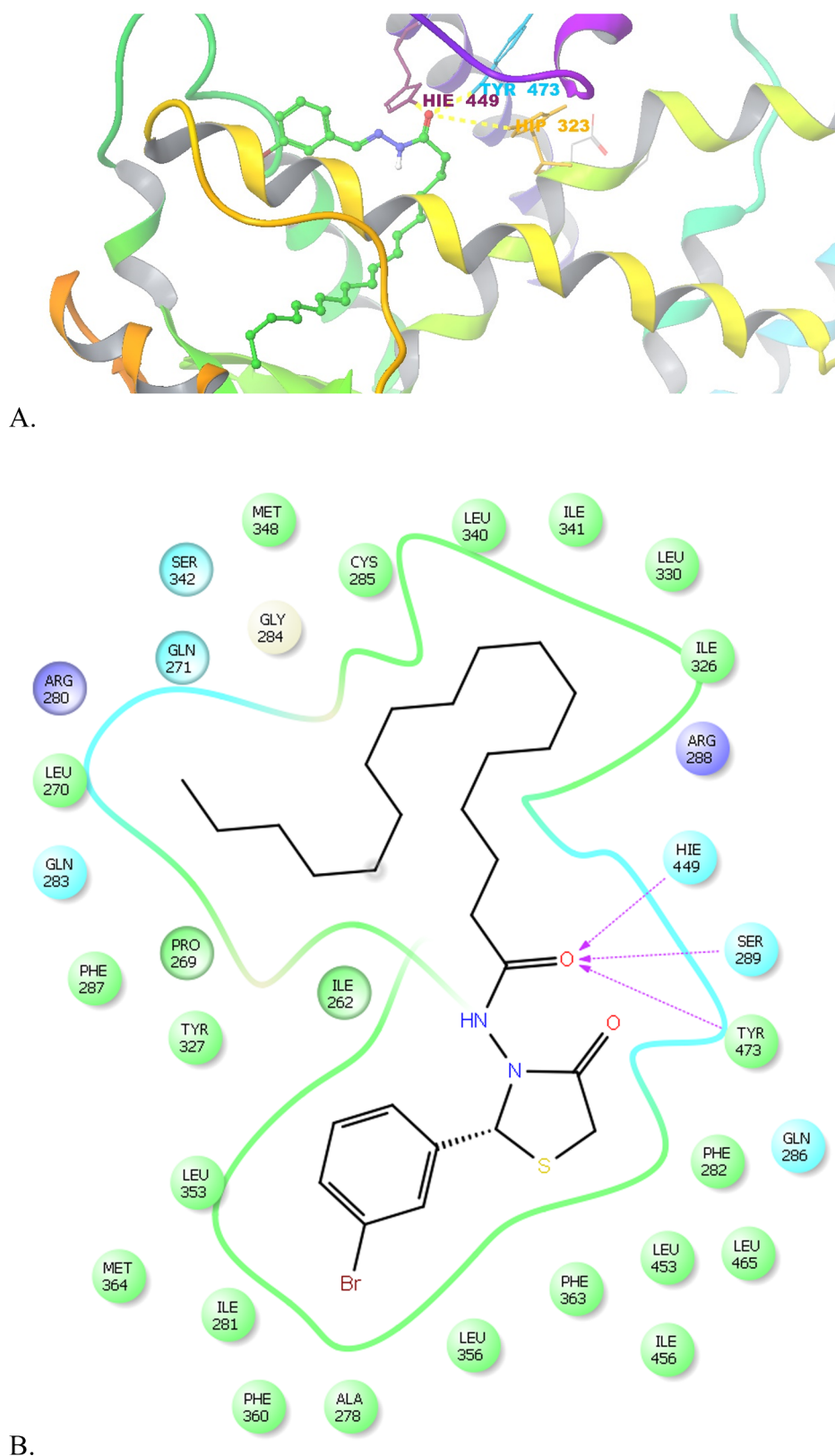


Fig. 2. (A) 3D interrelationship picture of S21 (PDB ID: 1FM9) presenting hydrogen bonds with yellow dot lines in relation to amino acid HIE 449, HIP 323 and TYR 473. (B) 2D docked picture of compound S21 showing hydrophobic interactions by green amino acid residues.

3.4. Structure activity relationship (SAR)

The consequences of biological actions of new analogs betrayed in-built anti-diabetic activity allied in fatty acid long chain nucleus and the

NH–N= linkage with different moieties. The new molecules contain various substituents on phenyl moiety at different positions which drop down the blood glucose level to less or more extent. Compound S21 containing bromo substituent which is electron withdrawing group

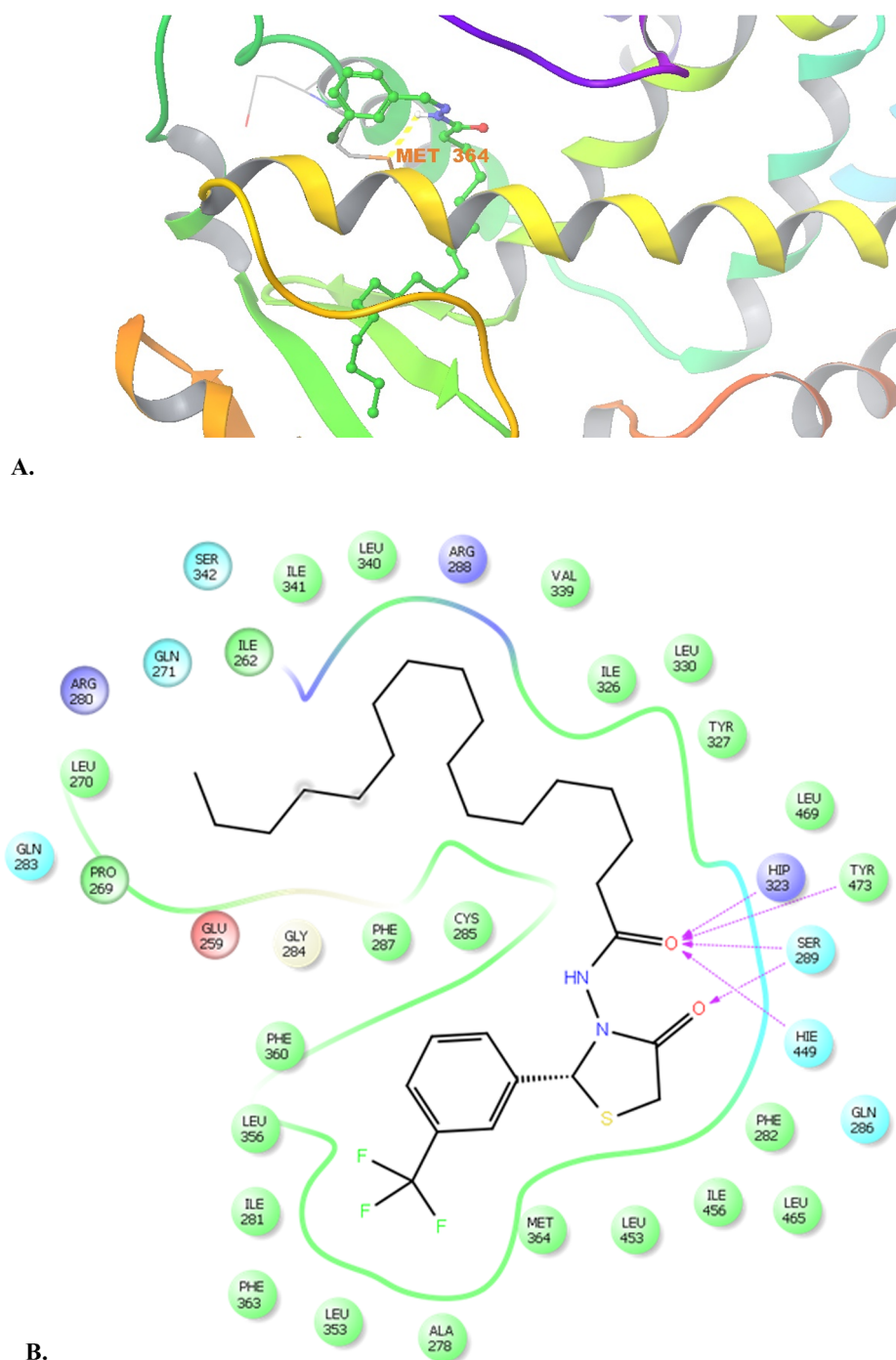


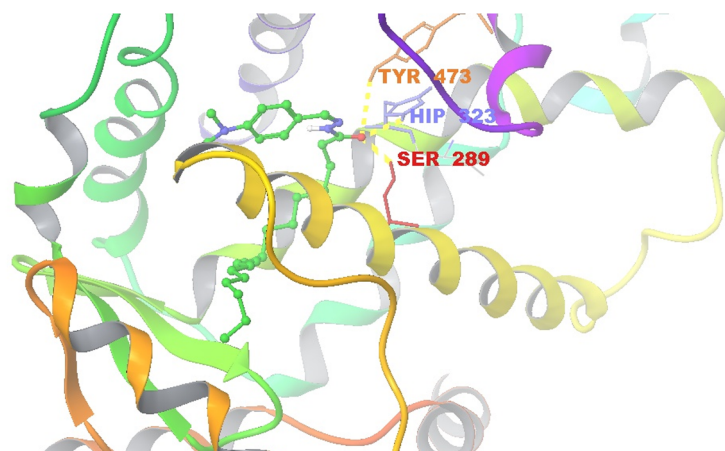
Fig. 3. (A) 3D interrelationship picture of **S10** (PDB ID: 1FM9) presenting hydrogen bonds with yellow dot lines in relation to amino acid MET 364. (B) 2D docked picture of compound **S10** showing hydrophobic interactions by green amino acid residues.

decreases the sugar level most significantly. This reduction was more than the standard pioglitazone. Entities showed less activity when phenyl ring was replaced with heterocycle moiety like furan. The presence of an electron withdrawing group like halogens on phenyl ring increases the anti-diabetic potential of the molecules. **S10** embodying chloro at meta position on phenyl ring was found to be second most active in reducing blood glucose level among tested compounds which was comparable to the standard. Pioglitazone reduced glucose level to 124.54 mg/dL after 6 h and **S10** suppresses to 130.08 mg/dL. **S7** was an exception in which weak electron donating group on phenyl ring i.e. dimethylamino gives salutary results in contrast to standard. It is noted that **S14** also accomplish electron withdrawing group on phenyl ring

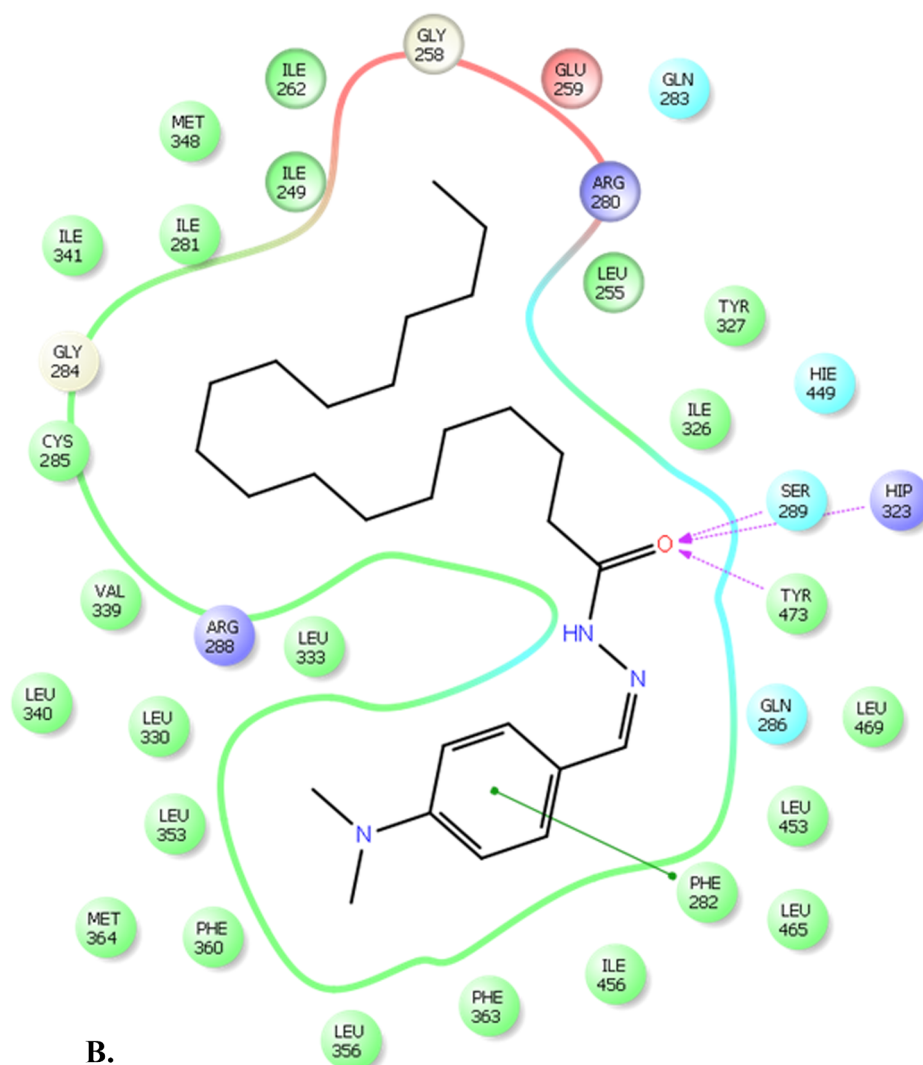
i.e. chloro group at para position contributing to an increase in activity by reducing glucose level. There was less activity when electron donating groups are substituent on phenyl ring as noticed in compounds **S4** and **S5** comprising 3,4 methoxy and 3,4,5 methoxy groups respectively when they are compared to standard and **S21**.

3.5. Discussion

The basis of this study is synthesis, docking and then estimating the selected entities to trigger reduction in glucose level in normal rats and anti-hyperglycaemic potential on rats induced with diabetes. These interpretations indicate the use of novel compounds as food



A.



B.

Fig. 4. (A) 3D interrelationship picture of **S7** (PDB ID: 1FM9) presenting hydrogen bonds with yellow dot lines in relation to amino acid TYR 473, HIP 323 and SER 289. (B) 2D docked picture of compound **S7** showing hydrophobic interactions by green amino acid residues and pi-pi interactions by green solid line.

supplements in diabetes. This work even though has visibly average reducing of glucose level in normal rats but the produced derivatives possess significant anti-hyperglycaemic potential on diabetic albino rats. Diabetes mellitus is initiated vigorously by streptozotocin, deadly

acting on β -cells which secrete insulin [37]. Hence STZ diabetes is indicated by rise in sugar level. Fatty acids are chief nutritional component involved in the cardiovascular and metabolic diseases [9]. Foods containing saturated fatty acids are also more preferable for the type 2

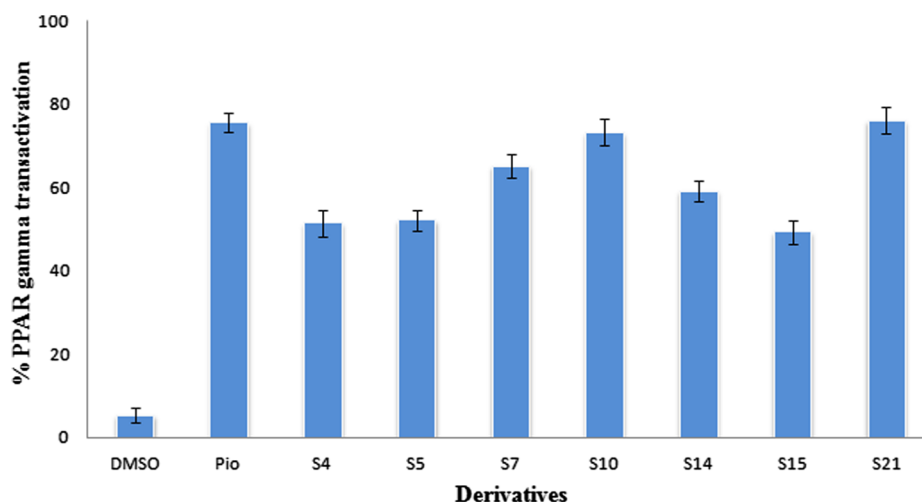


Fig. 5. Graphical representation of results of PPAR- γ transactivation assay. Values are expressed as mean \pm SEM by performing experiment three times in triplicate at 10 μ M.

Table 3

Cytotoxicity estimation of selected derivatives.

Compound code	Cytotoxicity against MCF-7 IC50 (μ M) ^a
S4	> 100
S5	> 100
S7	> 100
S10	> 100
S14	> 100
S15	> 100
S21	> 100
Etoposide (standard)	12.5 \pm 1.13

^a Values are expressed as mean \pm SD, every experiment was carried out at least three times.

Table 4

OGTT results in Normal Rats.

Normal rats Group	Dose taken	0 min	30 min	90 min
Normal control	0.1%CMC	82.21 \pm 0.57	168.05 \pm 2.75	124.55 \pm 4.01
Pioglitazone	36 mg/kg	88.77 \pm 2.32	161.85 \pm 3.29	101.05 \pm 1.14**
S4	100 mg/kg	86.96 \pm 3.10	169.4 \pm 4.06	111.77 \pm 2.56**
S5	100 mg/kg	85.5 \pm 1.69	167.36 \pm 3.06	110.87 \pm 2.53**
S7	100 mg/kg	83.7 \pm 2.00	164.95 \pm 3.31	104.68 \pm 1.50**
S10	100 mg/kg	83.32 \pm 2.08	162.37 \pm 2.51	103.26 \pm 2.95**
S14	100 mg/kg	84.73 \pm 2.57	165.9 \pm 3.24	107.13 \pm 1.50**
S15	100 mg/kg	89.8 \pm 1.85	170.15 \pm 2.13	112.8 \pm 2.37**
S21	100 mg/kg	84.95 \pm 1.57	160.82 \pm 2.86	99.92 \pm 1.71**

Data represent (n = 6) mean \pm SEM, analyzed comparing to control through one-way ANOVA and Dunnett's multiple comparison test.

** p < 0.01.

diabetic patients [10]. Recently it has been reported that substituted long chain fatty acids and its derivatives activate PPAR- γ [12]. As fatty acids are significant in treating type II diabetes, this invokes us to plan this study in search for the better anti-hyperglycaemic activities and safer profile than the available drugs.

Outcome is that the synthesized compounds have anti-hyperglycaemic efficacy according to the research papers published. The procedure of full mode of action requires more study. The results conclude that all derivatives reduce blood glucose level to standard range when prescribed for long duration. Our study is the only one presenting anti-hyperglycaemic activity of fatty acid. Surely further additional exploration in this view in diabetic individuals is aspired.

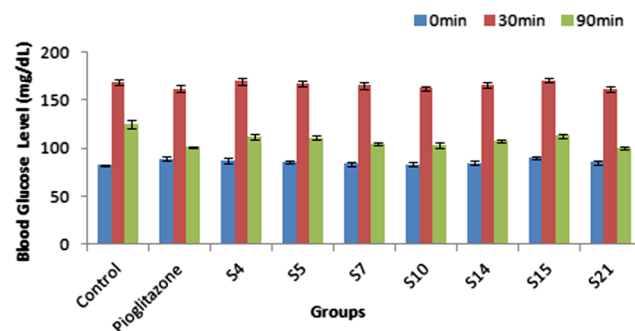


Fig. 6. Graphical representation of *in vivo* Oral Glucose Tolerance Test. Data represent (n = 6) mean \pm SEM, analyzed comparing to control through one-way ANOVA and Dunnett's multiple comparison test, ** p < 0.01.

Results of molecular docking performed on Maestro 9.0 software program (Schrodinger Inc. USA) indicates that compounds **S21**, **S10** and **S7** showed appreciable docking scores, -9.19 , -8.68 and -8.64 respectively and are properly positioned on the vital sites. The free binding energy lies between -80.54 and -53.79 kcal/mol remarkable comparing to standard (-51.58 kcal/mol). Compound **S21** was identified as most active among the synthesized derivatives and can be used lead candidate with excellent anti-hyperglycaemic activity due to presence of electron withdrawing group bromo. **S21** reduced the blood glucose level to 119.88 mg/dL in 6 h and the standard pioglitazone reduced the sugar level to 124.54 mg/dL. **S10** also indicated notably good activity as having electron withdrawing group chloro at meta position on phenyl ring. All other synthesized derivatives showed moderate anti-hyperglycaemic activity. Some derivatives showed low activity due to brief experimental time, so long period work may be required to get best results.

Hence, in view of docking and biological results, all the thirty derived compounds shows good activity with compound **S21** as most potent and thus can be further explored in search of potential new agents for type II diabetes. **S10** and **S7** could also act as lead to experiment its relevant therapeutic effect as anti-diabetic agent.

4. Conclusion

This research illustrates simple and efficient synthesis of novel Schiff base derivatives of fatty acid demonstrating outstanding anti-diabetic properties tested on albino wistar rats analogized with standard, pioglitazone. Moreover further scrutinization could be done on

Table 5
Anti-hyperglycaemic activity results in diabetic rats.

Diabetic rat group	Dose taken	0 h	2 h	4 h	6 h
Diabetic control	0.1%CMC	323.23 ± 2.36	316.98 ± 1.49	305.86 ± 1.56	291.73 ± 1.54
Pioglitazone	36 mg/kg	317.12 ± 2.51	196.13 ± 1.23	169.67 ± 1.54	124.53 ± 1.62**
S4	100 mg/kg	284.45 ± 2.68	182.5 ± 1.97	153.3 ± 3.04	113.33 ± 2.39**
S5	100 mg/kg	311.2 ± 2.35	203.12 ± 2.66	173.38 ± 2.45	131.16 ± 1.26**
S7	100 mg/kg	319.91 ± 3.87	196.45 ± 3.47	161.97 ± 2.15	128.55 ± 1.75**
S10	100 mg/kg	322.38 ± 1.18	201.33 ± 1.57	165.1 ± 3.83	130.08 ± 0.97**
S14	100 mg/kg	312.7 ± 3.86	201.38 ± 3.59	163.58 ± 4.78	124.5 ± 2.05**
S15	100 mg/kg	307 ± 1.42	194.7 ± 3.34	164.57 ± 2.1	138.26 ± 2.03**
S21	100 mg/kg	321.13 ± 1.18	191.96 ± 2.03	163.48 ± 2.63	119.88 ± 2.37**

Data represent (n = 6) mean ± SEM, analyzed comparing to control through one-way ANOVA and Dunnett's multiple comparison test.

** p < 0.01.

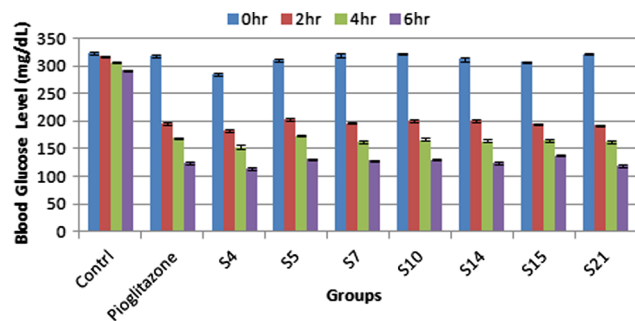


Fig. 7. Graphical representation of *in vivo* antihyperglycemic results. Data represent (n = 6) mean ± SEM, analyzed comparing to control through one-way ANOVA and Dunnett's multiple comparison test, ** p < 0.01.

these prominent analogs in discovering more potent and safer new agents for type 2 diabetes having proactive core for peroxisome proliferator activated receptor.

Conflict of interest

The authors declare no conflict of interest.

Acknowledgments

Ms. Garima Kapoor and Ms. Rubina Bhutani are indebted to DIPSAR, New Delhi, India for providing laboratory research facilities. We both are also thankful to Department of Science and technology, New Delhi, India (DST) (sanction order numbers DST/Inspire Fellow/2014/266 and DST/Inspire Fellow/2014/258 respectively), India for providing financial assistance in our research work.

Appendix A. Supplementary material

Supplementary data to this article can be found online at <https://doi.org/10.1016/j.bioorg.2018.12.004>.

References

- P. Thiriochana, N.C. Sahu, K. Hazra, S. Ramachandran, Synthesis and biological evaluation of new Thiaziazole analogues for anti-diabetic activity against Alloxan induced diabetes, *J. Pharm. Res.* 8 (2014) 1559–1562.
- N.C. Turner, J.C. Clapham, Insulin resistance, impaired glucose tolerance and non-insulin-dependent diabetes, pathological mechanisms and treatment: Current status and therapeutic possibilities, *Prog. Drug Res.* 51 (1998) 33–94.
- R. Bhutani, D.P. Pathak, G. Kapoor, A. Husain, R. Kant, Md.A. Iqbal, Synthesis, Molecular modelling studies and ADME prediction of benzothiazole clubbed oxadiazole-Mannich bases, and evaluation of their Anti-diabetic activity through *in vivo* model, *Bioorg. Chem.* 77 (2018) 6–15.
- Y. Itoh, Y. Kawamata, M. Harada, M. Kobayashi, R. Fujii, S. Fukusumi, K. Ogi, M. Hosoya, Y. Tanaka, H. Uejima, H. Tanaka, M. Maruyama, R. Satoh, S. Okubo, H. Kizawa, H. Komatsu, F. Matsumura, Y. Noguchi, T. Shinohara, S. Hinuma, Y. Fujisawa, M. Fujino, Free fatty acids regulate insulin secretion from pancreatic β cells through GPR40, *Nature* 22 (2003) 173–176.
- R. Murugan, S. Anbazhagan, S.S. Narayanan, Synthesis and *in vivo* antidiabetic activity of novel dispiropyrrolidines through [3+2] cycloaddition reactions with thiazolidinedione and rhodanine derivatives, *Eur. J. Med. Chem.* 44 (2009) 3272–3279.
- G. Kapoor, D.P. Pathak, R. Bhutani, A. Husain, S. Jain, R. Kant, Md.A. Iqbal, Newly synthesized oxadiazole based mannich base derivatives of fatty acid: *in silico* study and *in vivo* anti-hyperglycaemic estimation, *Orient. J. Chem.* 34 (5) (2018) 2253–2267.
- C. Wolfrum, C.M. Borrmann, T. Borchers, F. Spener, Fatty acids and hypolipidemic drugs regulate peroxisome proliferator-activated receptors α - and γ -mediated gene expression via liver fatty acid binding protein: A signaling path to the nucleus, *Proc. Natl. Acad. Sci.* 98 (2001) 2323–2328.
- S.A. Klierer, S.S. Sundseth, S.A. Jones, P.J. Brown, G.B. Wisely, C.S. Kobles, P. Devchand, W. Wahli, T.M. Willson, J.M. Lenhard, J.M. Lehmann, Fatty acids and eicosanoids regulate gene expression through direct interactions with peroxisome proliferator-activated receptors α and γ , *Proc. Natl. Acad. Sci.* 94 (1997) 4318–4323.
- K. Kotarsky, N.E. Nilsson, E. Flodgren, C. Owman, B. Olde, A human cell surface receptor activated by free fatty acids and thiazolidinedione drugs, *Biochem. Biophys. Res. Commun.* 301 (2003) 406–410.
- H. Storm, C. Thomsen, E.P. Rasmussen, C. Christiansen, K. Hermansen, Comparison of a carbohydrate-rich diet and diets rich in stearic or palmitic acid in NIPPM patients, *Diabetes Care* 20 (1997) 1807–1813.
- I.N. Kendrlish, Fatty acid oxidation inhibitors—a new class of antidiabetic drugs. I. Experimental study of hypoglycemic effect of bromstearic acid in comparison with daonil, *Probl. Endokrinol. (Mosk)* 26 (1980) 48–53.
- K. Schoonjans, B. Staels, J. Auwerx, Role of the peroxisome proliferator-activated receptor (PPAR) in mediating the effects of fibrates and fatty acids on gene expression, *J. Lipid Res.* 37 (1996) 907–925.
- F.J. Schopfer, M.P. Cole, A.L. Groeger, C. Chen, N.K.H. Khoo, S.R. Woodcock, F.G. Bisello, U.N. Motanya, Y. Li, J. Zhang, M.T. Garcia-Barrio, T.K. Rudolph, V. Rudolph, G. Bonacci, P.R.S. Baker, H.E. Xu, C.I. Batthyany, Y.E. Chen, T.M. Hallis, B.A. Freeman, Covalent peroxisome proliferator-activated receptor γ adduction by nitro-fatty acids, *J. Biol. Chem.* 285 (2010) 12321–12333.
- E.A. Elzahany, K.H. Hegab, S.K.H. Khalil, N.S. Youssef, Synthesis, characterization and biological activity of some transition metal complexes with schiff bases derived from 2-formylindole, salicylaldehyde, and N-amino rhodanine, *AJBAS* 2 (2008) 210–220.
- N. Sari, Antibacterial activities of some new amino acid-schiff bases, *G.U. J. Sci.* 16 (2003) 283–288.
- R.S. Joseyphus, M.S. Nair, Antibacterial and Antifungal Studies on Some Schiff Base Complexes of Zinc(II), *Mycobiology* 36 (2008) 93–98.
- C. Yuan, L. Lu, X. Gao, Y. Wu, M. Guo, Y. Li, X. Fu, M. Zhu, Ternary oxovanadium (IV) complexes of ONO-donor Schiff base and polypyridyl derivatives as protein tyrosine phosphatase inhibitors: synthesis, characterization, and biological activities, *J. Biol. Inorg. Chem.* 14 (2009) 841–851.
- C. Jaiganesh, V.R. Devi, S.I. Pillai, S. Subramanian, Synthesis, characterization and evaluation of antidiabetic properties of a new metformin-3-hydroxyflavone complex studied in high fat diet fed - low dose streptozotocin induced experimental type 2 diabetes in wistar rats, *Int. J. Pharm. Bio. Sci.* 8 (2017) 1–15.
- E.M. Hodnett, P.D. Mooney, Antitumor activities of some Schiff bases, *J. Med. Chem.* 13 (1970).
- M.M. Abd-Elzaher, A.A. Labib, H.A. Mousa, S.A. Moustafa, M.M. Ali, A.A. El-rashedy, Synthesis, anticancer activity and molecular Docking study of Schiff base complexes Containing thiazole moiety, *BJBAS* 5 (2016) 85–96.
- S. Zhu, S. Xu, J. Wang, Z. Zhao, J. Jiang, Synthesis and Herbicidal Activities of p-Menth-3-en-1-amine and Its Schiff Base Derivatives, *J. Agric. Food Chem.* (2016), <https://doi.org/10.1021/acs.jafc.6b03977>.
- A. Kumar, J. Fernandes, P. Kumar, Synthesis, antimicrobial and anti-inflammatory studies of some novel Schiff Base Derivatives, *Int. J. Drug Dev. & Res.* 6 (2014) 165–171.
- S. Adisakwattana, Cinnamic acid and its derivatives: mechanisms for prevention and management of diabetes and its complications, *Nutrients* 9 (2017) 163.
- S. Sujarani, T.A. Sironmani, A. Ramu, Synthesis, characterization and toxicity studies of schiff bases [2-(2, 2-diphenylethylimino)methyl]phenols] anchored silver

- nanoparticles, Dig. J. Nanomater. Biostruct. 7 (2012) 1843–1857.
- [25] A. Rauf, M.R. Bandaya, R.H. Mattoo, Synthesis, characterization and antimicrobial activity of long-chain hydrazones, Acta Chim. Slov. 55 (2008) 448–452.
- [26] P.P. Naik, R.R. Somani, S.O. Waghulde, P. Juvatkar, P.Y. Shirodkar, M.K. Kale, Synthesis and biological activities of some 1, 3, 4-oxadiazole based schiff's bases, Int. J. Pharm. Phytopharmacol. Res. 3 (2013) 222–225.
- [27] K.M. Daoud, S.R. Mohammed, Z.F. Saeed, Synthesis and antibacterial activity of 2-cinnamyl-5-substituted- 1,3,4-oxadiazole, 1,3,4-thiadiazoles and 5-cinnamyl-3-substituted- 1,2,4-triazoles, Nat. J. Chem. 25 (2007) 102–110.
- [28] Molinspiration software or free molecular property calculation services. Available from URL: www.molinspiration.com/cgi-bin/properties (last accessed 21.05.17).
- [29] M.R. Ali, S. Kumar, O. Afzal, N. Shalmali, W. Ali, M. Sharma, S. Bawa, 12-Benzamido-4-methylthiazole-5-carboxylic acid derivatives as potential xanthine oxidase inhibitors and free radical scavengers, Arch. Pharm. Chem. Life Sci. 350 (2017) 1–13.
- [30] M.M.D. Silva, M. Comin, T.S. Duarte, M.A. Foglio, J.E.D. Carvalho, M.D.C. Vieira, A.S.N. Formagio, Synthesis, antiproliferative activity and molecular properties predictions of galloyl derivatives, Molecules 20 (2015) 5360–5373.
- [31] C.A. Lipinski, F. Lombardo, B.W. Dominy, P.J. Feeney, Experimental and computational approaches to estimate solubility and permeability in drug discovery and development settings, Adv. Drug. Deliver Rev. 23 (1997) 4–25.
- [32] V. Obermoser, M.E. Urban, M.S. Murgueitio, G. Wolber, U. Kintscher, R. Gust, New telmisartan-derived PPAR γ agonists: Impact of the 3D-binding mode on the pharmacological profile, Eur. J. Med. Chem. 124 (2016) 138–152.
- [33] D. Yadav, A.A. Chaudhary, V. Garg, M.F. Anwar, M.M. Rahman, S.S. Jamil, H.A. Khan, M. Asif, In vitro toxicity and antidiabetic activity of a newly developed polyherbal formulation (MAC-ST/001) in streptozotocin-induced diabetic Wistar rats, Protoplasma 250 (2013) 741–749.
- [34] V.R. Avupati, R.P. Yejella, A. Akula, G.S. Guntuku, B.R. Doddi, V.R. Vutla, S.R. Anagani, L.S. Adimulam, A.K. Vyrricharla, Synthesis, characterization and biological evaluation of some novel 2,4-thiazolidinediones as potential cytotoxic, antimicrobial and antihyperglycemic agents, Bioorg. Med. Chem. Lett. 22 (2012) 6442–6450.
- [35] R.B.S. Kumar, B. Kar, N. Dolai, A. Bala, P.K. Haldar, Evaluation of anti-hyperglycemic and antioxidant properties of *Streblus asper* Lour against streptozotocin-induced diabetes in rats, Asian Pac. J. Trop. Dis. (2012) 139–143.
- [36] C. Lee, H.S. Lee, Y.J. Cha, W.H. Joo, D.O. Kang, J.Y. Moon, In vivo investigation of anti-diabetic properties of ripe onion juice in normal and streptozotocin-induced diabetic rats, Prev. Nutr. Food Sci. 18 (2013) 169–174.
- [37] S. Sen, B. De, T.S. Easwari, Synthesized 2-substituted-3-phenylthiazolidine-4-ones as potent antioxidants and antidiabetic agents, Trop. J. Pharm. Res. 13 (2014) 1445–1454.
- [38] K. Jain, S. Malviya, A.K. Gupta, A. Kharia, Design, synthesis and biological evaluation of glycogen synthase kinase-3 β inhibitors as antidiabetic agents, IJPSR 5 (2014) 5025–5041.
- [39] S. Nazreen, M.S. Alam, H. Hamid, M.S. Yar, S. Shafi, A. Dhulap, P. Alam, M.A.Q. Pasha, S. Bano, M.M. Alam, S. Haider, Y. Ali, C. Kharbanda, K.K. Pillai, Design, synthesis, in silicomolecular docking and biological evaluation of novel oxadiazole based thiazolidine-2,4-diones bis-heterocycles as PPAR-g agonists, Eur. J. Med. Chem. 87 (2014) 175–185.
- [40] E.S. Al-Abdullah, H.M. Al-Tuwaijri, H.M. Hassan, M.E. Haiba, E.E. Habiband, A.A. El-Emam, Antimicrobial and hypoglycemic activities of novel *n*-mannichbases derived from 5-(1-adamantyl)-4-substituted-1,2,4-triazoline-3-thiones, Int. J. Mol. Sci. 15 (2014) 22995–23010.
- [41] S. Ramachandran, A. Rajasekaran, N. Adhirajan, In Vivo and In Vitro antidiabetic activity of *Terminalia paniculata* bark: an evaluation of possible phytoconstituents and mechanisms for blood glucose control in diabetes, 20 (2015) pp. 5360–5373.
- [42] Z. Ali, M.J. Akhtar, A.A. Siddiqui, A.A. Khan, M.R. Haiderand, M.S. Yar, Design, synthesis, and biological evaluation of novel quinazolineclubbed thiazoline derivatives, Arch. Pharm. Chem Life Sci. 349 (2017) 1–11.